Comunicações Geológicas

Comunicações Geológicas (2025) 112, 1, 35-58
ISSN: 0873-948X; **e-ISSN:** 1647-581X

Miragaia longicollum MG 4863: New fossil and historical evidence from the most complete stegosaur from Europe

Miragaia longicollum MG 4863: Expandindo o conhecimento do Estegossauro mais completo da Europa

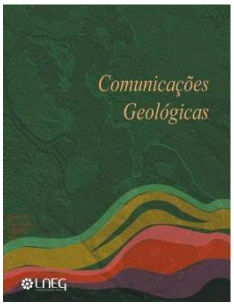

F. Costa [1,2*], S. C. R. Maidment[3], C. Sequero[4], V. D. Crespo[1,2]

DOI: https://doi.org/10.34637/xs1n-3d27
Recebido em 24/06/2025 / Aceite em 10/10/2025
Publicado online em outubro de 2025

Artigo original
Original article

Abstract: Additional historical data regarding the original finding and excavation (circa 1958-1959) of the *Miragaia longicollum* stegosaur MG 4863 has been identified (including field notes and the complete field map), allowing a better understanding of its stratigraphic context. Additionally, osteological material that was previously partially encased in matrix was fully prepared and restored, including anterior and posterior caudal vertebrae, metacarpals, and five semi-complete dorsal vertebrae (the latter being the most significant addition, as these are the only skeletal elements shared by all type specimens of dacentrurine taxa).

New anatomical information from these additional elements provides further evidence that *M. longicollum* is distinct from the closely related Late Jurassic stegosaur *Dacentrurus armatus* from England (demonstrated mainly by various caudal differences).

The newly prepared material further completes what was already the best reference specimen among the Dacentrurinae clade, as well as Stegosauria in Europe during the Late Jurassic, increasing its value to better understand these contexts in future studies.

Keywords: Dacentrurinae, Stratigraphy, Upper Jurassic, Taxonomy, historical record.

Resumo: Informação histórica adicional da recolha do espécime MG 4863 de *Miragaia longicollum* foi localizada (incluindo notas de campo e o mapa de campo completo), permitindo uma melhor compreensão do seu contexto estratigráfico. Além disso, material osteológico que anteriormente estava parcialmente encapsulado em matriz foi preparado e restaurado, incluindo vértebras caudais anteriores e posteriores, metacarpos, e cinco vértebras dorsais semi-completas (sendo estas últimas a adição mais significativa, dado serem os únicos elementos esqueléticos partilhados por todos os espécimes-tipo de estegossauros Dacentrurinos).

Novas informações anatómicas destes elementos adicionais fornecem evidências adicionais que *M. longicollum* é distinto do estegossauro aparentado *Dacentrurus armatus* do Jurássico Superior de Inglaterra (demonstrado principalmente por várias diferenças caudais).

O material recentemente preparado completa ainda mais aquele que já era o melhor espécime de referência no clado Dacentrurinae, bem como Stegosauria na Europa durante o Jurássico Superior, aumentando o seu valor para melhor compreender estes contextos em estudos futuros.

Palavras-chave: Dacentrurinae, Estratigrafia, Jurássico Superior, Taxonomia, registo histórico.

1 GeoBioTec, Departamento de Ciências da Terra, Faculdade de Ciências e Tecnologia, Universidade NOVA Lisboa, Campus Caparica. 2829-516 Caparica, Portugal.

2 Museu da Lourinhã, Rua João Luís de Moura 95, 2530-158, Lourinhã, Portugal.

3 Fossil Reptiles, Amphibians and Birds Section, The Natural History Museum, Cromwell Road, London SW7 5BD, UK.

4 Departamento de Geodinámica, Estratigrafía y Paleontología, Universidad Complutense de Madrid, C. José Antonio Novais, 12 Ciudad Universitaria 28040 Madrid, Spain.

* Corresponding author / Autor correspondente: fj.pinto@campus.fct.unl.pt

Introduction

Miragaia longicollum Mateus *et al.,* 2009 is known from the Lusitanian Basin (Late Jurassic, west Portugal), characterized for having an exceptionally long neck with at least 17 cervical vertebrae and long caudal dermal spines (over one metre long in life; Costa and Mateus, 2019; Mateus *et al.,* 2009). The holotype (ML 433; Fig. 1b) was discovered in 2001 near the eponymous village of Miragaia (Lourinhã, Portugal) in the upper Kimmeridgian-lower Tithonian beds of the Lourinhã formation (Praia Azul member; Araújo *et al.,* 2009; Mateus *et al.,* 2009, 2017) and consists of an almost complete anterior half of the skeleton. A referred juvenile specimen (ML 433-A; Fig. 1a) was found associated with the holotype and includes dorsal vertebrae and pelvic material (Mateus *et al.,* 2009). Later another specimen (MG 4863; Fig. 1c) housed and exhibited at Museu Geológico de Lisboa (LNEG) was ascribed to *M. longicollum.*

Closely related to the *Miragaia* genus is *Dacentrurus armatus* (Owen, 1875), the holotype of which (NHMUK PV OR 46013) was found in the lower Kimmeridge Clay Formation (Upper Jurassic) of Swindon, Wiltshire (England; Galton, 1985, 1991). In Mateus *et al.* (2009), *Miragaia* and *Dacentrurus* were found as sister taxa forming the clade named therein as Dacentrurinae, sister clade to Stegosaurinae, and defined as all stegosaurs closer to *D. armatus* than *Stegosaurus stenops* Marsh, 1887. Other taxa have since been found as dacentrurines (or closer to *D. armatus* than other stegosaur species), namely the North American stegosaur *Alcovasaurus* (= *Miragaia*) *longispinus* (Gilmore, 1914) from the Upper Jurassic Morrison Formation of Wyoming (USA; see Costa and Mateus, 2019, and Galton and Carpenter, 2016), *Adratiklit boulahfa* Maidment *et al.,* 2020, and *Thyreosaurus atlasicus*

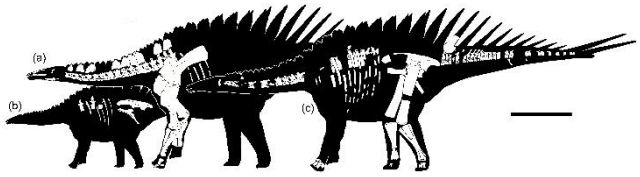

Figure 1. Skeletons of *Miragaia longicollum* specimens. (a) ML 433; (b) ML 433-A; modified from Mateus *et al*., 2009, and Costa and Mateus, 2019; scale bar equal to 1 metre.

Figura 1. Esqueletos de exemplares de *Miragaia longicollum*. (a) ML 433; (b) ML 433-A; modificado de Mateus *et al.,* 2009, e Costa e Mateus, 2019; barra de escala igual a 1 metro.

Zafaty *et al.,* 2024, both the latter from the Middle Jurassic El Mers III Formation of Morocco (Maidment *et al,* 2020; Raven *et al.,* 2023; Zafaty *et al.,* 2024). In some analyses, however, *Miragaia* has been found closer to taxa other than *Dacentrurus* (and not within a Dacentrurinae clade), such as closest to *Hesperosaurus mjosi* Carpenter *et al.*, 2001 (Dai *et al.,* 2022; Raven and Maidment, 2017; Zafaty *et al.,* 2024), or *Adratiklit boulahfa* Maidment *et al.,* 2020.

Additional dacentrurine fossils (including partial specimens ascribed to *Dacentrurus* sp. or *D. armatus*; see Maidment *et al.,* 2008) include occurrences from the Late Jurassic to Early Cretaceous of England (*e.g*. Galton, 1985; Owen, 1877), France (*e.g*. Allain *et al*., 2022; Galton, 1991; Nopcsa, 1911), Portugal (*e.g*. Escaso et al., 2007; Galton, 1991; Lapparent and Zbyszewski, 1957), Spain (*e.g*. Casanovas-Cladellas *et al*., 1995; Cobos *et al*., 2010; Company *et al*., 2010; Pereda-Suberbiola *et al*., 2003; Ruiz-Omeñaca, 2000; Ruiz-Omeñaca *et al*., 2013; Sánchez-Fenollosa *et al*., 2024) and the USA (Costa and Mateus, 2019, 2023). Dacentrurines represent the most common record of stegosaurs in Europe, and the former appears to have been one of the most successful groups of non-avian dinosaurs in Iberia during the Upper Jurassic (Cobos *et al.,* 2010; Guillaume *et al*., 2022; Maidment *et al.,* 2020). The *M. longicollum* specimen MG 4863 is a partial skeleton from Atouguia da Baleia (Peniche, Portugal), (Fig. 2) found in the late 1950s but only studied since 2015 (Costa *et al.*, 2017, 2019). It comprises 35 vertebrae (10 cervical, 5 dorsal, and 25 caudal), two chevrons, left pelvis, both hindlimbs, metacarpals, radiale, a partial caudal spine, and diverse fragments (including of the skull, cervical plates, ribs, and various other vertebrae), making it the most complete stegosaur skeleton from Europe, as well as the most complete dacentrurine discovered to date (Costa and Mateus, 2019). After descriptions and comparisons of this specimen (Costa and Mateus, 2019), at least 27 morphological differences from the holotype of *D. armatus* were identified, 10 of which also present in the *M. longicollum* holotype (see Costa and Mateus, 2019; Costa and Crespo, 2025), demonstrating the validity of *M. longicollum* as a distinct species from *D. armatus*, which has been a matter of debate among authors (*e.g*. Cobos *et al.,* 2010; Escaso, 2014; Ortega *et al.,* 2009). A more recent proposal of a synonymization of *M. longicollum* with *D. armatus* (Sánchez-Fenollosa *et al*., 2024) omitted to acknowledge or discuss the majority of the diagnostic differences of MG 4863 from the holotype of the latter, unsubstantiating such a proposal (see Discussion for more details). Costa and Mateus (2019) also concluded that all but one of the diagnostic characters of *Alcovasaurus longispinus* (*sensu* Galton and Carpenter, 2016; based on Gilmore, 1914) occurred in MG 4836 (among other uniquely shared traits), leading to the proposal that *A. longispinus* belonged to the genus *Miragaia* as *Miragaia longispinus* (see Costa and Mateus, 2019). Recognizing *M. longispinus* as a dacentrurine provided an explanation for how its morphology (clearly dispar from the coeval *S. stenops* and *H. mjosi*) had confounded researchers for more than a century (*e.g.* Galton, 2016; Galton and Carpenter, 2016; Gilmore, 1914; Olshevsky and Ford, 1993; Raven and Maidment, 2017; Ulansky, 2014). This also results in *Miragaia* being so far the only genus of non-avian dinosaur named in Portugal, with fossils from other countries being later revealed to also belong to the genus (showcasing the palaeontological research made in Portugal; Costa and Crespo, 2025; Costa and Mateus, 2019). The combination of the osteological material of MG 4863 with ML 433 and ML 433-A also made *M. longicollum* osteologically one of the best represented stegosaur taxa known currently in the world (Galton and Upchurch, 2004).

Given the clear scientific significance of MG 4836, the purpose of the current contribution is to document and describe the newly prepared fossil material from it, and to provide recently discovered new information regarding the locality of its discovery.

Material and Methods

The material of MG 4863 presented here is that which, due to technical restrictions of mechanical laboratory preparation, could not be completely freed from the matrix or reconstructed by the time of a previous comprehensive description of the specimen (Costa and Mateus, 2019). These skeletal elements include dorsal vertebrae, anterior caudal vertebrae, and metacarpals. Revisions and corrections from previous work are informed mainly by first-hand comparisons with the holotype of *D. armatus* (NHMUK PV OR 46013), newer stegosaur material described since the original description of MG 4863 (*e.g.* Dai *et al.,* 2022; Maidment *et al.,* 2020; Sánchez-Fenollosa *et al*., 2024; Zafaty *et al.,* 2024), and first-hand comparisons with other stegosaur specimens (referenced by the collection number of the respective specimens).

The additional preparation also resulted in some elements being reconstructed differently (such as smaller parts being found to attach to more complete skeletal elements; see (Figs. 3-12), and Costa and Mateus, 2019: figures 22-25, 32-35, 48, 49, 65, 66). An updated list of the skeletal elements of MG 4863 is annexed (Appendix 1).

New data on the discovery locality of MG 4863

Georges Zbyszewski (1909-1999) was responsible for the geological mapping of central-west Portugal from 1942 to 1979 for SGP and IGM (currently LNEG), resulting also in the discovery of almost every dinosaur fossil in the collection of MG (Lapparent and Zbyszewski, 1957; Costa and Mateus, 2019). This included the specimen MG 4863, which by 2015 was stored in the Alfragide campus of LNEG with just the label "Atouguia da Baleia". The specimen was supposedly collected in 1959 at the only location near Atouguia da Baleia marked in the 1:50 000 Geologic Map of Peniche (França and Zbyszewski, 1960: sheet 26-C; Fig. 2b, c) as "main deposit of possible dinosaur remains", 1 km NE from the centre of Atouguia da Baleia (for more details, see Costa *et al.*, 2017, 2019).

However, subsequent archival research has resulted in new discoveries which shed important new light on the discovery site of the specimen. This includes a field notebook belonging to Georges Zbyszewski containing four pages of notes about the collection of the "*Dinosaure du C. do Cervantes (Atouguia da Baleia*)", including lists and illustrations of some of the material,

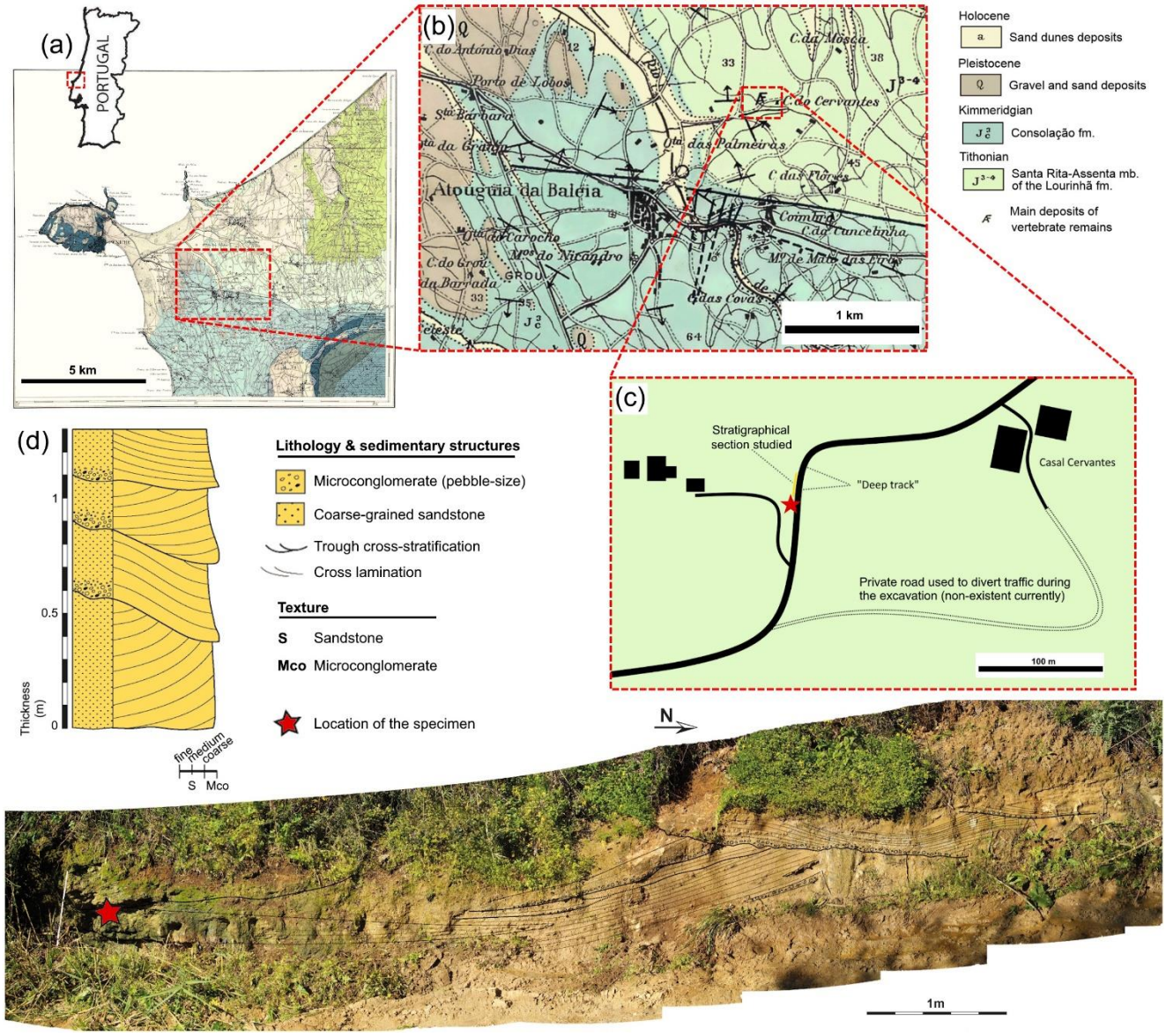

Figure 2. Geological context of the locality of *Miragaia longicollum* MG 4863. (a) simplified map of Portugal (top) and Sheet 26–C Peniche of Geologic Map of Portugal at scale 1:50 000, (França *et al.*, 1960); (b) detail of (a) with the centre of Atouguia da Baleia and nearby location marked as "main deposit of possible dinosaur remains", and simplified label (adapted *sensu* Mateus *et al.,* 2017); (c) Casal Cervantes area (detailed *circa* 1958 based on historic documents and personal reports); (d) lithostratigraphy and stratigraphic section of the site of MG 4863.

Figura 2. Enquadramento geológico da localidade de *Miragaia longicollum* MG 4863. (a) mapa simplificado de Portugal (em cima) e Folha 26–C Peniche da Carta Geológico de Portugal à escala 1:50 000 (França *et al*., 1960); (b) pormenor de (a) com o centro de Atouguia da Baleia e localização adjacente assinalada como "principal depósito de possíveis restos de dinossauros", e etiqueta simplificada (adaptado *sensu* Mateus *et al*., 2017); (c) área de Casal Cervantes (detalhada *circa* 1958 com base em documentos históricos e relatos pessoais); (d) litoestratigrafia e secção estratigráfica (em baixo) do sítio de MG 4863.

and a short description of the collection site and its stratigraphy (Appendix 2a, b). "Casal de Cervantes" is the residence closest to the location previously inferred to be the site of MG 4863, approximately 150 metres east from this location. This notebook is undated and handwritten in French, so not all its information could be deciphered or translated (Appendix 2c). Some unprepared matrix blocks and fossils are illustrated or labelled (Appendix 2b, c), some of which can be correlated to the fossils of MG 4863 (including by numbering applied in red crayon on the fossils, present prior to preparation; Appendix 3a-e). This notebook was previously in a private collection but is now housed in Museum da Lourinhã.

A personal communication was given in 2023 to one of the authors (FC) by Luís Filipe Silva, born in 1956 and raised in Casal Cervantes. Mr. Silva indicated an excavated depression in a road-cut where he recalled that a dinosaur was collected during his early youth and pointed out that throughout the years, he observed it deteriorate and eventually be covered up by vegetation (as was its state in 2023; Appendix 3h). This concavity (about 1.5 metres wide and tall and half a metre deep into the outcrop) has various 20-30 cm wide and nearly right-angled incisions, dissimilar to natural surface erosion, but congruent with filed work prospection with chisels and hammers to detach large blocks of matrix from the outcrop. Mr. Silva also noted that the road section north adjacent

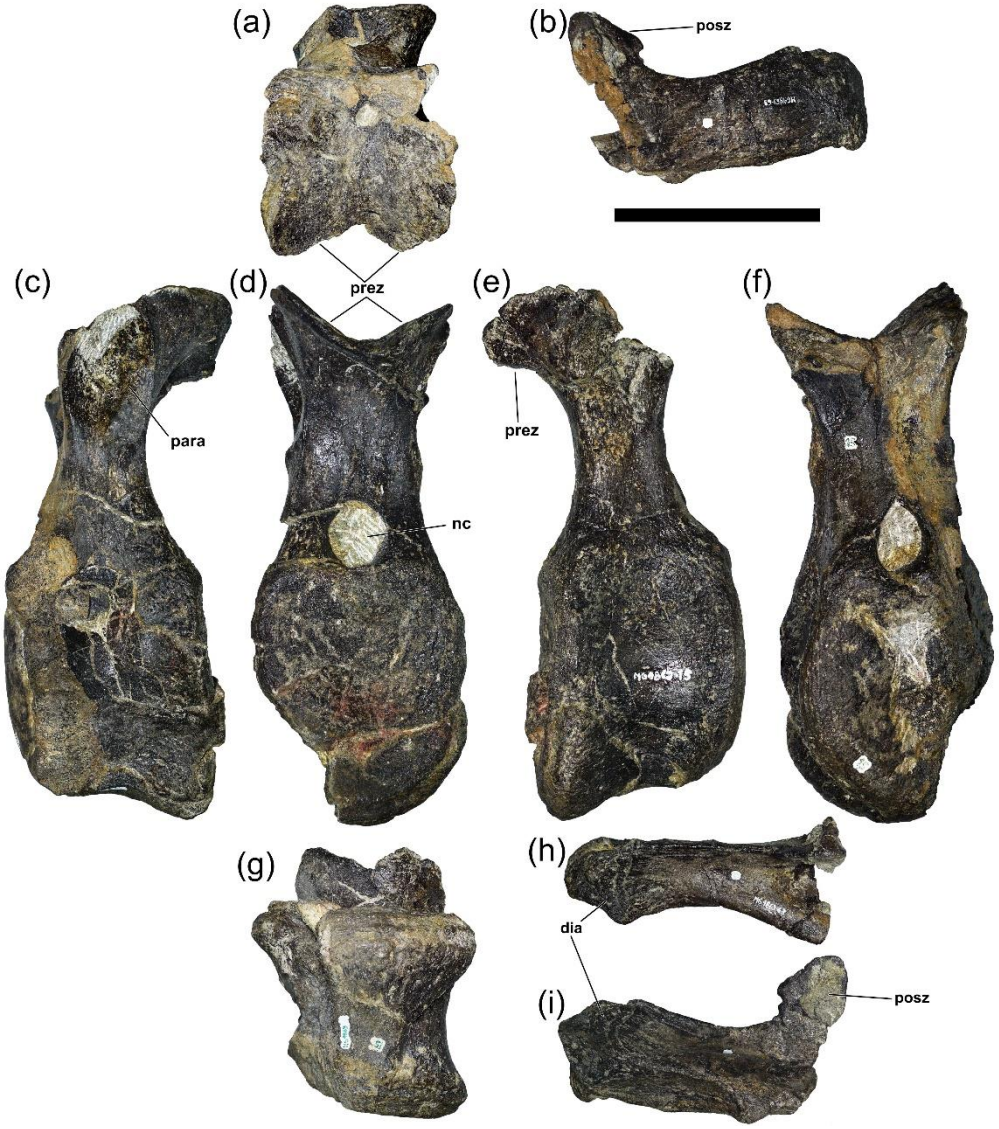

Figure 3. Dorsal vertebra two and three of *Miragaia longicollum* MG 4863. (a, c-g) MG 4863-15 (D3); (b, h, i) MG 4863-63 (D2); in (a, b) dorsal, (c) right lateral, (d) anterior, (e) left lateral, (f, h) posterior, and (g, I) ventral views; key: dia, diapophyses; nc, neural canal; para, parapophyses; posz, postzygapophyses; prez, prezygapophyses; scale bar equal to 10 cm.

Figura 3. Vértebras dorsais dois e três de *Miragaia longicollum* MG 4863. (a, c-g) MG 4863-15 (D3); (b, h, i) MG 4863-63 (D2); em vista (a, b) dorsal, (c) lateral direita, (d) anterior, (e) lateral esquerda, (f, h) posterior e (g, I) ventral; dia, diapófises; nc, canal neural; para, parapófises; posz, pós-zigapófises; prez, pré-zigapófises; barra de escala igual a 10 cm.

to the dig site (south of a sharp right-hand turn; Fig. 2c) was much more steeply inclined and deep at the time of extraction of the fossil remains (close to 20º or 30º degrees), which correlates with the description by Zbyszewski in his field notes (Appendix 2b, c).

A note by Zbyszewski dated 28th December 1958 from the archives of IGM (AHGM) was discovered, in which he states to have arranged to produce a second edition of his memoir "*Les Dinosauriens du Portugal*" (Lapparent and Zbyszewski, 1957), specifying this to be mainly to include the "skeletal parts found in the excavations undergone near Atouguia da Baleia, in the sandstones of the Lusitanian" (Appendix 3g). It was previously postulated that MG 4863 was collected in 1959 (Costa *et al.*, 2017) mainly because Atouguia da Baleia is only specifically listed in 1959 as one of the areas where geologic survey was being conducted by IGM (Mota, 2007: page 219). Given that the note by Zbyszewski dated to latest 1958 (and the absence of the Atouguia da Baleia stegosaur in Lapparent and Zbyszewski, 1957), it is most likely that this specimen was found sometime in 1958. An extension of the geological fieldwork in the region to collect the specimen is congruent with the "intensified geological survey work" by SGP documented for 1959 for Peniche (Mota, 2007: page 219), despite having been listed as "concluded or almost concluded" in 1958 (Mota, 2007: pp. 212-213).

A complete quarry map of the dig-site, referring to the Casal Cervantes dinosaur, was also discovered in the IGM archives (AHGM PT LNEGSG02.01.275; Appendix 4). Copies of the illustrations in the field notes by Zbyszewski are also part of this quarry map, as are the some of the skeletal elements identified as therein (Appendix 2a-c). However, given that the specimen has been fully prepared and reconstructed, resulting in labelling written over having been mostly removed or lost, the contribution of the quarry map to contextualizing the material is limited at this point.

The information sourced from these newly accessed field notes, personal communications, observable geological context of the alleged site, matrix and osteology of the collected specimen, as well as other historical documents previously considered are congruent with each other. Consequently, it is now clear that the stegosaur from Atouguia da Baleia (MG 4863) was found in 1958 by Georges Zbyszewski in a roadcut on the west side of a dirt road (39°20'45.1"N 9°18'58.3"W; Fig. 2d), approximately 1 km NE

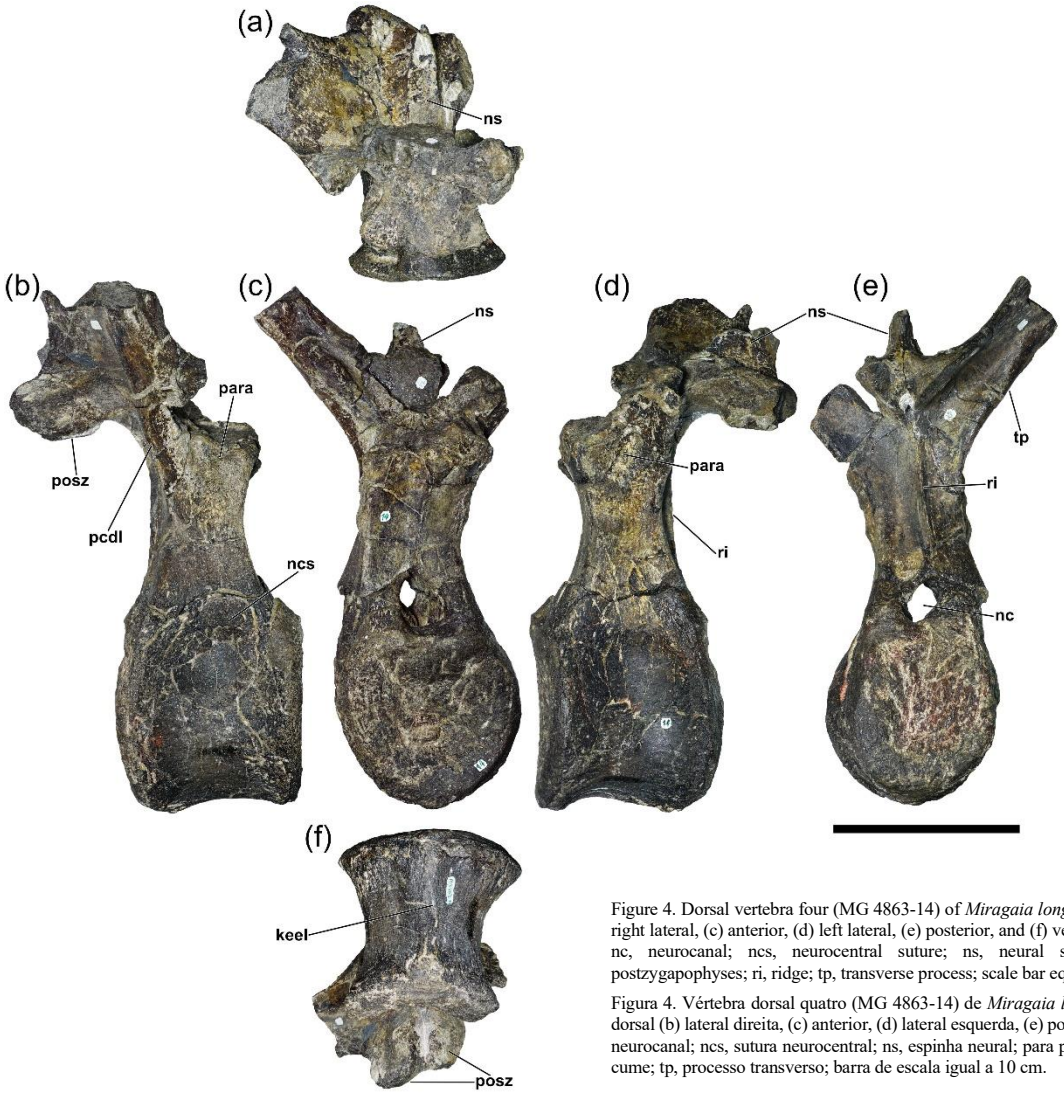

Figure 4. Dorsal vertebra four (MG 4863-14) of *Miragaia longicollum* MG 4863. In (a) dorsal (b) right lateral, (c) anterior, (d) left lateral, (e) posterior, and (f) ventral views; key: keel, ventral keel; nc, neurocanal; ncs, neurocentral suture; ns, neural spine; para, parapophysis; posz, postzygapophyses; ri, ridge; tp, transverse process; scale bar equal to 10 cm.

Figura 4. Vértebra dorsal quatro (MG 4863-14) de *Miragaia longicollum* MG 4863. Em vista (a) dorsal (b) lateral direita, (c) anterior, (d) lateral esquerda, (e) posterior e (f) ventral; keel, quilha; nc, neurocanal; ncs, sutura neurocentral; ns, espinha neural; para parapófise; posz, pós-zigapófises; ri, cume; tp, processo transverso; barra de escala igual a 10 cm.

from the centre of Atouguia da Baleia (Peniche, Portugal), and 150 m west of Casal Cervantes.

With this, an outcrop over 10 metres long north adjacent to the dig site has also been identified (Fig. 2d), allowing a more detailed sedimentological study undertaken (see below).

Geological context

These deposits correspond to the Upper Jurassic (Kimmeridgian-Tithonian; Hill, 1989) Lourinhã formation, a siliciclastic unit that represents alluvial fan and fluvio-deltaic environments, with intercalations of estuarine and lagoon events, deposited in the Lusitanian Basin (Hill, 1988, 1989; Leinfelder and Wilson, 1989; Taylor *et al*., 2014).

The 1.3 m thick outcrop North-adjacent to the site and analysed here (Fig. 2d) corresponds to trough cross-stratified and cross-laminated coarse-grained sandstones with intercalation of microconglomerate (pebble-size) beds, arranged in several amalgamated channelled bodies with a lateral extent of 2-5 m and up to 30-60 cm thick. These channelled bodies show a fining-upwards structure, with pebble-sized microconglomerates at their base (intervals of few centimetres thick) grading upwards into coarse-grained sandstones, in some cases with some of the pebble-sized grains intercalated. These deposits are interpreted as a multilateral fluvial channel fill, with the amalgamated channelized bodies representing successive lateral channel migrations (Taylor *et al*. 2014).

The stratigraphy of the putative site is compatible with the observable sedimentological features of the matrix of MG 4863 and the description in the notes by Zbyszewski (Appendix 2b, c), corroborating these as the same. The deposits in which the specimen was found are part of the beds identified in the Geologic Map of Peniche (Portugal) at scale 1:50 000 (Sheet 26–C Peniche; França *et al.*, 1960) as "$J_{3\text{-}4}$—Upper sandstones with plant and dinosaur fossils", described therein as muddy sandstones with intercalations of mudstones and marls, with some conglomerate layers with limestone elements in the base of the complex.

Based on the available cartographies in the literature (*e.g.* França *et al.*, 1960, 1961; Mannupella,1999; Taylor et al., 2014; Zbyszewski *et al.,* 1966), these deposits can be reviewed to be part of the uppermost Kimmeridgian Praia da Amoreira-Porto Novo Member (*sensu* Mateus *et al.,* 2017; São Bernardino Member *sensu* Taylor *et al.,* 2014), but this correlation is expected to be more precise with future studies with a deeper analysis of the Lusitanian Basin.

Description and comparisons

Dorsal vertebrae

Five semi-complete dorsal vertebrae are known in MG 4863, three of which preserved semi-articulated (having since been separated during preparation; Figs. 5, 6, 7a-f), and the other two isolated (Figs. 3a, c-g, 4). These are here identified as the 3rd, 4th, and 6th to 8th dorsal vertebrae (generally each one position more posteriorly than previously interpreted; see Costa and Mateus, 2019) after comparisons to other stegosaurs with better-preserved dorsal series (e.g., *S. stenops*, NHMUK PV R 36730, USNM 4934; Maidment *et al*. 2015). Various fragments of previously uncertain assignment were also found to attach or pertain to these vertebrae, further completing them (see Figs. 4, 6, 7a-f; Costa and Mateus, 2019: figures 22, 23, 25). D6 (MG 4863-17; Fig. 5) is the most complete dorsal vertebra, lacking only the prezygapophyses. A left dorsal transverse process with the postzygapophysis (MG 4863-63; Fig. 3b, h, i) is most likely part of D2 (but could be part of D3, although it could not be found to unequivocally attach to it), while a fragment of a transverse process (found to have fossilized articulated posteriorly to that of D8) is all the preserved material of D9 (MG 4863-113; Fig. 7g-i).

All the dorsal centra are wider transversely than long anteroposteriorly (Tab. 1), as in the holotype of *Miragaia longicollum* (ML 433; ML 433A; Mateus *et al*., 2009), *Dacentrurus armatus* (NHMUK PV OR 46013; Owen 1875, Galton 1985; Galton, 1991), *Adratiklit boulahfa* (Maidment *et al*., 2020) and *Thyreosaurus atlasicus* (Zafaty *et al.* 2024). This contrasts to other stegosaur taxa, which had dorsal centra longer than wide or equidimensional (e.g., *Stegosaurus stenops, Kentrosaurus aethiopicus* Hennig, 1915*, Huayangosaurus taibaii* Dong *et al*., 1982*, Loricatosaurus priscus* (Nopcsa, 1911)*, Hesperosaurus mjosi, Gigantspinosaurus sichuanensis* Ouyang, 1992*, Chungkingosaurus jiangbeiensis* Dong *et al*., 1983*, Tuojiangosaurus multispinus Dong* et *al., 1977, Wuerhosaurus homheni* Dong, 1973*, Bashanosaurus primitivus* Dai *et al*., 2022, and *Yanbeilong ultimus* Jia *et al*., 2024 (Carpenter *et al*., 2001; Dai *et al*., 2022; Dong, 1993; Dong *et al*., 1977, 1983; Galton, 1982, 1985, 1990; Gilmore, 1914; Hao *et al*., 2018; Hennig, 1915; Maidment and Wei, 2006, Maidment et al., 2015; Zhou, 1984). The posterior articular facets in MG 4863 are slightly wider transversely than the anterior facets (except for D4, which is much narrower posteriorly, but this seems to have been exaggerated by taphonomic compression; Fig. 4). The centra become proportionately wider passing posteriorly in the series, from approximately 1.1 times wider than long in D3 to 1.5 and 1.35 times wider in D7 and D8 (Tab. 1). This condition of becoming wider towards the last two-thirds of the dorsal series is analogous to *D. armatus* (NHMUK PV OR 46013; Galton and Upchurch, 2004) and opposite to the condition in *S. stenops*, where the dorsal vertebrae become more elongated from D1 to D7 (only in the most posterior becoming slightly less elongated; Maidment *et al*., 2015). The anterior dorsal centra of MG 4863 are about one third the height of the vertebrae if complete, becoming closer to a fourth the height passing posteriorly in the preserved series (Tab. 1).

The articular facets of the centra are flat to slightly concave, as in most stegosaurs (Galton and Upchurch, 2004), but appear

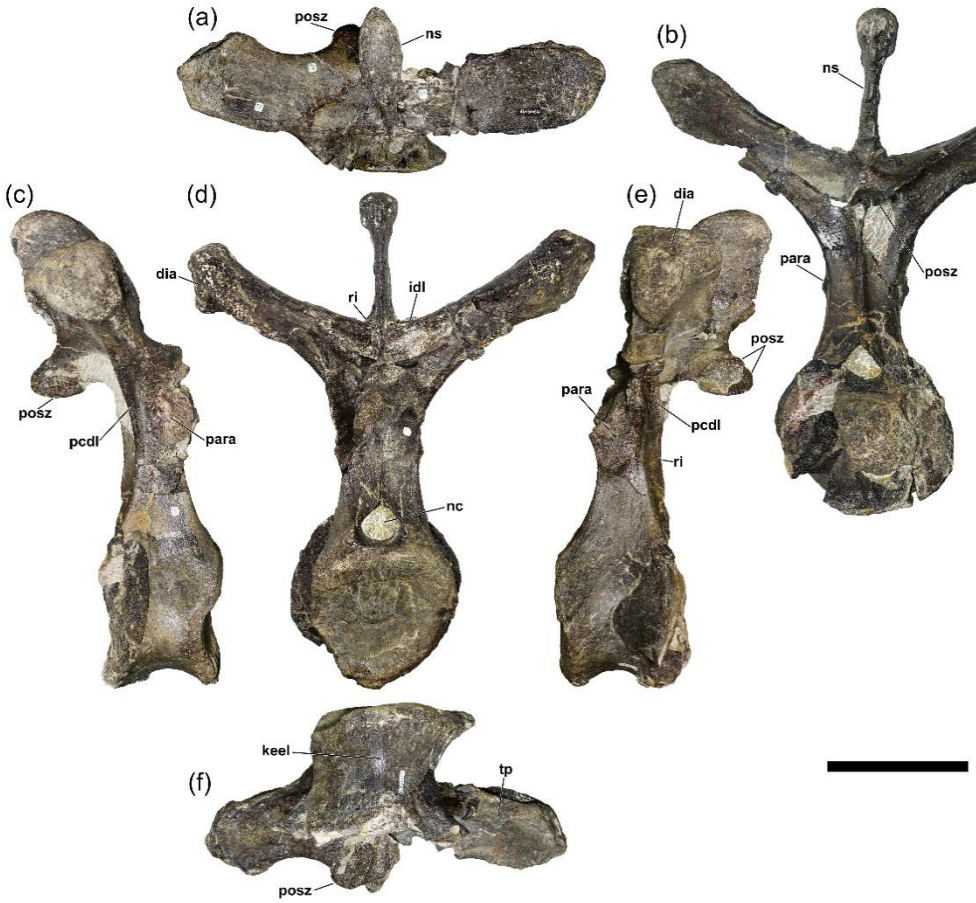

Figure 5. Dorsal vertebra six (MG 4863-17) of *Miragaia longicollum* MG 4863. In (a) dorsal, (b) right lateral, (c) anterior, (d) left lateral, (e) posterior, and (f) ventral views; key: dia, diapophysis; idl, interdiapophyseal lamina; keel, ventral keel; nc, neurocanal; ns, neural spine; para, parapophysis; pcdl, posterior centrodiapophyseal lamina; posz, postzygapophyses; prez, prezygapophyses; ri, ridge; tp, transverse process; scale bar equal to 10 cm.

Figura 5. Vértebra dorsal seis (MG 4863-17) de *Miragaia longicollum* MG 4863. Em vista (a) dorsal, (b) lateral direita, (c) anterior, (d) lateral esquerda, (e) posterior e (f) ventral; dia, diapófise; idl, lâmina interdiapofisal; keel, quilha; nc, neurocanal; ns, espinha neural; para, parapófise; pcdl, lâmina centrodiapofisal posterior; posz, pós-zigapófises; prez, pré-zigapófises; ri, cume; tp, processo transverso; barra de escala igual a 10 cm.

Table 1. Measurements of dorsal vertebrae of *Miragaia longicollum* MG 4863. D, dorsal vertebrae; values represent the maximum measurement; ( ) incomplete measurement (inferior to actual measurement if fossil was complete); * estimated measurement; values in mm.

Tabela 1. Medidas das vértebras dorsais de *Miragaia longicollum* MG 4863. D, vértebras dorsais; os valores representam a medida máxima; ( ) medida incompleta (inferior à medida real se o fóssil estivesse completo); * medida estimada; valores em mm.

	Total height	Centrum Length	Centrum height (anterior, posterior)	Centrum width (anterior, posterior)
D3	(230)	89	120, 110	102, 100
D4	(280)	95	101, 101	90*, 103
D6	360	95	98, 100	124, 107
D7	(260)	80*	99*, 115*	121*, 124
D8	(320)	85	98*, 99	114*, 116

slightly flatter posteriorly in D3, D4 and D7 (likely exaggerated by deformation in the latter; Figs. 3f, 4e, 6h). In outline the centra are sub-circular in anterior and posterior views, but the subtle longitudinal keel present ventrally in all centra may give the appearance of a sharper ellipsoid-outline ventrally in the cases where the centrum borders are not well preserved (such as D6 and D8; Figs. 5d, 7d). A ventral keel is present on the dorsal vertebrae of the holotype of *M. longicollum* (ML 433) and *T. atlasicus* (Mateus *et al*., 2009; Zafaty *et al*., 2024). In contrast, many stegosaurs lack a keel on the dorsal centra, including *S. stenops*, *B. primitivus*, *Y. ultimus* and *D. armatus* (Dai *et al*., 2022; Galton, 1985; Jia *et al*., 2024; Maidment *et al*., 2015). In lateral view the ventral surface is slightly concave. The centra are spool-shaped in ventral view, with lateral sides gently to markedly concave (Figs. 3-7), as in the holotype of *M. longicollum* (ML 433), *D. armatus*, *A. boulahfa* and *T. atlasicus* (Galton, 1985; Maidment *et al*. 2020; Mateus *et al*., 2009; Sánchez-Fenollosa *et al*., 2024; Zafaty *et al*., 2024). The sides are more concave just ventral to the neurocentral

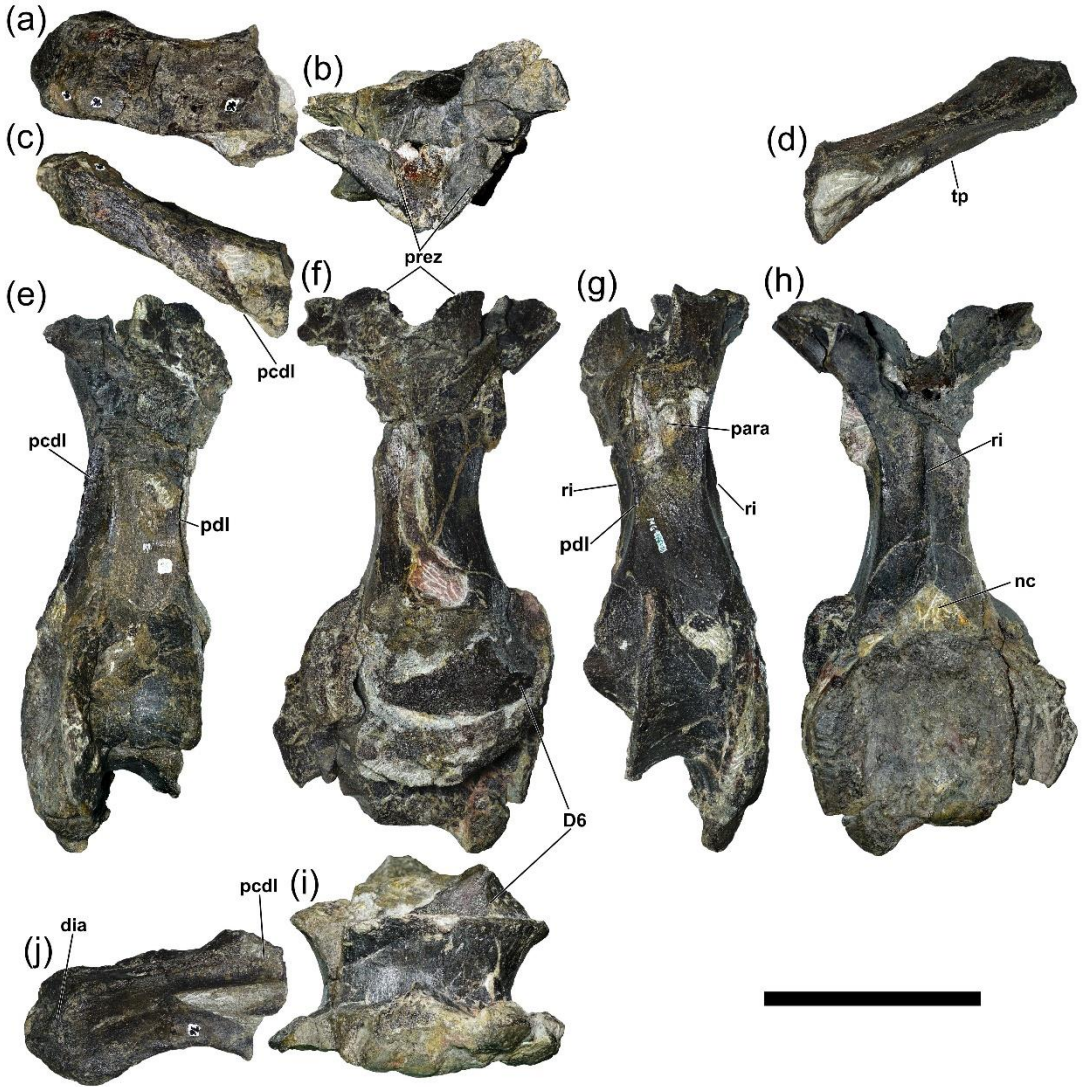

Figure 6. Dorsal vertebrae seven (MG 4863-16) of *Miragaia longicollum* MG 4863. In (a, b) dorsal, (c, f) anterior, (d, h) posterior, (e) right lateral, (g) left lateral, and (i, j) ventral views; (a, c, d, j); key: D6, ventroposterior margin of centrum of the sixth dorsal vertebra; dia, diapophysis; nc, neurocanal; para, parapophyses; pcdl, posterior centrodiapophyseal lamina; pdl, paradiapophyseal lamina; prez, prezygapophyses; ri, ridge; tp, transverse process; scale bar equal to 10 cm.

Figura 6. Vértebra dorsal sete (MG 4863-16) de *Miragaia longicollum* MG 4863. Em vista (a, b) dorsal, (c, f) anterior, (d, h) posterior, (e) lateral direita, (g) lateral esquerda e (i, j) ventral; D6, margem ventroposterior do centro da sexta vértebra dorsal; (a, c, d, j) processo transverso, dia, diapófise; nc, neurocanal; para, parapófises; pcdl, lâmina centrodiapofisal posterior; pdl, lâmina paradiapofisal; prez, pré-zigapófises; ri, cume; tp, processo transverso; barra de escala igual a 10 cm.

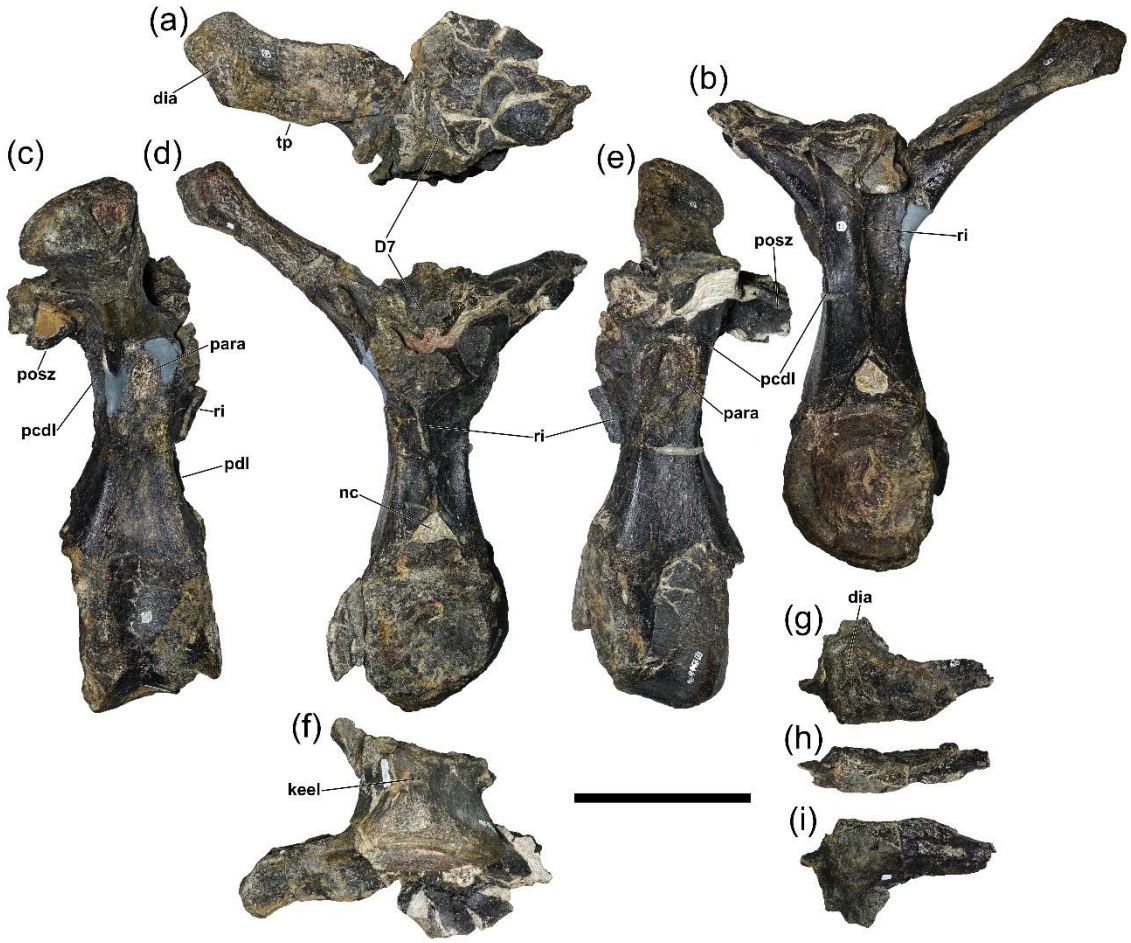

Figure 7. Dorsal vertebrae eight and nine of *Miragaia longicollum* MG 4863. (a-f), MG 4863-13 (D8), (g-i) MG 4863-113 (D9), in (a, g) dorsal, (b) right lateral, (c, h) anterior, (d) left lateral, (e) posterior, and (f, i) ventral views; key: D7, postzygapophyses of dorsal vertebra seven; dia, diapophysis; keel, ventral keel; nc, neurocanal; para, parapophysis; pcdl, posterior centrodiapophyseal lamina; pdl, paradiapophyseal lamina; posz, postzygapophyses; ri, ridge; scale bar equal to 10 cm.

Figura 7. Vértebras dorsais oito e nove de *Miragaia longicollum* MG 4863. (a-f), MG 4863-13 (D8), (g-i) MG 4863-113 (D9), em vista (a, g) dorsal, (b) lateral direita, (c, h) anterior, (d) lateral esquerda, (e) posterior e (f, i) ventral; D7, pós-zigapófises da vértebra dorsal sete; dia, diapófise; keel, quilha; nc, neurocanal; para, parapófise; pcdl, lâmina centrodiapofisal posterior; pdl, lâmina paradiapofisal; posz, pós-zigapófises; ri, cume; barra de escala igual a 10 cm.

suture (Figs. 4b, 6e, 7c, e), like in *A. boulahfa*, *T*, *atlasicus*, and *D. armatus* (markedly deeper in the latter; Galton, 1985; Maidment *et al*. 2020; Sánchez-Fenollosa *et al*., 2024; Zafaty *et al*., 2024). The anterior centrum edges of D7 were fractured and dislocated posterodorsally by taphonomic compression (Fig. 6e, g), while part of the posteroventral margin of the centrum of D6 are bonded to the anterior centrum of D7 (Fig. 6f, g, i). The anterior articular facet of the centrum of D3 extends deeper ventrally than the posterior facet (120 and 110 mm tall dorsoventrally respectively), as in two of the centra of *T. atlasicus* (Zafaty *et al.,* 2024).

The neural arch pedicels (including the column dorsal to the neural canal, measured from the floor of the neural canal to the base of the neural spine) are slightly over 1.5 times the height of the centrum (Figs. 3-7), similar to *D. armatus*, *A. boulahfa* and *T. atlasicus* (Galton, 1985; Maidment *et al.,* 2020; Zafaty *et al.,* 2024), but differing from stegosaurs with much taller neural arches (such as *S. stenops*, *W. homheni*, *C. jiangbeiensis*, *L. priscus*, *K. aethiopicus*, *T. multispinus* and *Y. ultimus*; Galton and Upchurch, 2004; Jia *et al.,* 2024), while other stegosaurs have much shorter pedicels, not dorsally elongated above the neural canal (such as *H. taibaii*, *H. mjosi*, *G. sichuanensis, B. primitivus* and *Baiyinosaurus baojiensis* Li *et al*., 2024 (Carpenter *et al*., 2001; Dai *et al.,* 2022; Hao *et al*., 2018; Li *et al*., 2024; Maidment and Wei, 2006). The pedicels become increasingly elongated dorsally passing posteriorly, as in other stegosaurs where known, including in *D. armatus* (Galton, 1985; Sánchez-Fenollosa *et al*., 2024). However, D8 is marginally shorter than D7, suggesting a slight height decrease of the most posterior dorsal pedicels, as also occurs in *S. stenops* between D10 and D13 (Maidment *et al*., 2015). The neural arch of D6 (the only complete one in height) is 2.6 times the height of the centrum measured from the floor of the neural canal to the dorsal edge of the neural spine (Tab. 1), as in *T. atlasicus* (Zafaty *et al.,* 2024) and *D. armatus* (NHMUK PV OR 46013; Galton, 1985). The pedicel is slightly taller in MG 4863-14 than MG 4863-15, so the former is more posterior (respectively D4 and D3; Figs. 3a, c-g; 4).

The posterior midline ridge of the neural arch (extending from dorsal to the neural canal onto the base of the postzygapophyses) is sharp and very consistently expanded (about 10 mm in all those preserved; Figs. 4d, e, 5e, 6g, 7b). The equivalent anterior ridge (extending from dorsal to the neural canal onto the base of the prezygapophyses) increasingly protrudes passing posteriorly in the dorsal vertebral series: it is absent in D3 (the anterior surface is even slightly concave just ventral to the prezygapophyses; Fig. 3d), almost indistinguishable in D4 and D6 (Figs. 4c, 5d), about as protruding as the posterior ridge in D7 (Fig. 6f, g), and much more

expanded than the posterior in D8 (Fig. 7c-e). Similar ridges in *S. stenops* are only distinct from D7 to D9 (Maidment *et al.,* 2015), indistinct in most dorsal vertebrae of *D. armatus* (NHMUK PV OR 46013; Galton, 1985), markedly developed in *A. boulahfa* and flanked by two shallow fossae (Maidment *et al.,* 2020), and absent in *H. mjosi* (Maidment *et al*., 2018).

The anterior and posterior boundary silhouettes of the neural canal are tear drop-shaped, with a sharp tip dorsally (where it meets respectively the anterior and posterior midline ridges), but internally it narrows to a rounder outline in anterior view (Figs. 4c, E, 5b, d, 7b). In D8 the neural canal appears to be very flattened ventrally and smaller in anterior view, but this is due to part of the broken dorsoposterior edge of the centrum from D7 covering it partially (Fig. 7d). In anterior view, the neural canals are a third to less than a third the width and height of the centrum, smaller than in other stegosaurs, including *D. armatus* and *T. atlasicus* (Galton, 1985; Zafaty *et al.,* 2024), where these are generally over half the width and height of the centrum (Galton and Upchurch, 2004). This difference parallels the mid and posterior caudal neural arches (Costa and Mateus, 2019: figures 36-47), which in MG4863 are also a third or less the centrum width, while in *D. armatus* these are half or more (NHMUK PV OR 46013; Costa and Mateus, 2019).

The parapophyses are positioned at the intersection of the top of the pedicel and the base of the transverse process, are oval, slightly concave facets, taller dorsoventrally than long anteroposteriorly, with protruding rugose borders. As the parapophyses in MG 4863-14 are further dorsally positioned from the suture line than in MG 4863-15, the former is more posterior the vertebral series (Figs. 4, 5).

D3 is the only dorsal vertebra with almost complete and undeformed prezygapophyses (Fig. 3a, c-e), which are large, sub-rounded in dorsomedial view, slightly longer anteroposteriorly than dorsoventrally tall, and extend slightly beyond the anterior articular facet of the centrum. They face dorsomedially (Fig. 3d, f) at a slightly more obtuse angle than the postzygapophyses in D4 and D6 (and face more medially than the anterior dorsal vertebrae of *S. stenops*, which face mostly dorsally; Maidment *et al*., 2015). The anterior edges of the prezygapophyses of D3 merge with the interprezygapophyseal lamina in a single gently curved "V" shaped anterior border (Fig. 3d). In dorsal view, they are gently bifurcated anteriorly (Fig. 3a), but are connected by more than half of the length of the articular facets, as in the holotype of *M. longicollum* (ML 433; Mateus *et al.,* 2009). D7 is the only other dorsal vertebra with prezygapophyses, but these are strongly deformed by compression, facing posteriorly (Fig. 6f, g). In both D3 and D7 the prezygapophyses do not possess a dorsal process on the posterior region of the lateral margins, unlike *A. boulahfa* and a specimen referred to *D. armatus* (Maidment *et al*., 2020; Sánchez-Fenollosa *et al*., 2024).

Posteroventral to the prezygapophyses, there is a strongly concave platform in dorsal view (an intraprezygapophyseal shelf), which is bordered posterodorsally by a vertical surface formed by the connection of the transverse processes anteromedially (present in most other stegosaurs; Galton and Upchurch, 2004; Figs. 4c, 5d). This large concavity is obscured in lateral view by the prezygadiapophyseal laminae. The almost horizontal dorsal surface between the transverse processes is intersected by a sharp and prominent ridge that extends ventrally down the anterior surface of the neural spine, terminating on the midline level with the posteriormost extend of the prezygapophyses. This gives this area a "cross" shape in anterior view (Fig. 5d), similarly to *T. atlasicus* and *S. stenops* (Maidment *et al*., 2015; Zafaty *et al.,* 2024; Fig. 5d), but unlike the condition in *A. boulahfa*, where this midline ridge bifurcates level with the top of the prezygapophyses and merges again a short distance dorsally (Maidment *et al.,* 2020).

In posterior view, the postzygapophyses unite ventromedially in a "V" shaped wedge, but with a marked rounded notch ventrally (Figs. 4e, 5b, 7d), as in *D. armatus* and *H. taibaii* (Galton and Upchurch, 2004). This ventral notch extends dorsoposteriorly, so in dorsal view the articular surfaces of the postzygapophyses are separated by a bifurcation of the posterior margins, most distinctly in D4 (also present in D2 and D6, but less conspicuous due to only one postzygapophysis being complete; Figs. 3b, i, 4a, f, 5f). In other stegosaurs (including *H. mjosi* and *S. stenops*; Carpenter *et al.*, 2001; Galton, 1985; Maidment *et al.*, 2015), the postzygapophyses are indistinguishably fused in dorsal and ventral view. The dorsal surface of the postzygapophyses is contiguous with the dorsal surface of the transverse processes and adjacent to the base of the neural spine posteriorly. The postzygapophyseal articular facets are oval in D4 and much larger than in the more posterior vertebrae, where they are also more lenticular in outline (Figs. 4-7). The postzygapophyses extend posteriorly, with the articular facets placed wholly beyond to the posterior articular facet of the centrum, hanging from a bridge between them and the pedicels that is ventrally concave in lateral view (Figs. 4b, d, 5c, e, 7c, e).

The posterior centrodiapophyseal lamina (PCDL; Maidment *et al*., 2015; Wilson, 1999) passes posteriorly to the parapophyses (Fig. 4c, 5b-e), and gives a T-shaped cross-section to the transverse processes, similarly to *T. atlasicus* and *D. armatus* (Galton, 1985; Sánchez-Fenollosa *et al*., 2024; Zafaty *et al.,* 2024). A paradiapophyseal lamina is also present, but it is not as prominent as the PCDL, and is almost flat where it meets the top of the parapophyses (Figs. 5, 7). Anterior centroparapophyseal laminae (ACPL) are present but not as distinct or markedly projecting as the PCDL, and unlike *A. boulahfa* and *S. stenops* where the ACPL are more conspicuous (Maidment *et al*., 2015, 2020). ACPL are not present in *D. armatus* and *T. atlasicus*, but a low process may extend ventrally from the parapophyses (without continuity until the centra; Galton, 1985; Zafaty *et al*., 2024: page 351; NHMUK PV OR 46013).

The transverse processes project dorsolaterally and closer to horizontal than vertical, averaging 30-35º with the horizontal, as in *D. armatus*, *T. atlasicus*, *G. sichuanensis,* as well as the holotype of *M. longicollum* (Galton, 1985; 1991; Hao *et al.,* 2018; Mateus *et al*., 2009; Zafaty *et al.,* 2024), while in other stegosaurs these are typically upturned over 50° above the horizontal (Carpenter *et al*., 2001; Dai *et al*., 2022; Dong *et al*., 1977; Galton and Upchurch, 2004; Jia *et al.,* 2014; Ostrom and McIntosh, 1966). The angle of the transverse processes of MG 4863 appears to be closest to horizontal by the mid-dorsal vertebrae (similarly to *D. armatus;* Sánchez-Fenollosa *et al*., 2024), approximately 45º with the horizontal in D4, 25° in D6, and 35° in D8. This is opposite of that which is observed in most stegosaurs (such as *S. stenops, L. priscus,* and *H. mjosi;* Carpenter *et al*. 2001; Maidment *et al.,* 2008, 2015, 2018; Sánchez-Fenollosa *et al*., 2024), where the transverse processes become increasingly elevated relative to the horizontal from the anterior to the mid-dorsal vertebrae, and reduce in elevation passing to the most posterior dorsal vertebrae (Maidment *et al*., 2015). In MG 4863, the transverse processes are slightly curved posteriorly, so the anterior margin is gently convex while the posterior is gently concave (Figs. 3-7).

The articular surfaces of the diapophyses are broad anteroposteriorly and convex in anterior and dorsal view, sub-triangular in outline in lateral view, and delimited dorsally by a rugose surface with fibres oriented axially (Figs. 3-7).

Only D6 preserves a complete neural spine (Fig. 5), but D4, D7 and D8 preserve part of their bases (Figs. 4a, c, 9a, d). The neural spine is offset posteriorly from the pedicel, so in lateral view the anterior margin of the neural spine is almost continuous vertically with the posterior margin of the pedicel column (Figs. 4b, 5c). The neural spine is transversely thin and axially long, approximately 80 mm long in D6, sub-rectangular in lateral view, with the anterior and posterior margins parallel and straight. The spine apex in D6 expands transversely and gradually from about two thirds its height, to over double the width of the rest of the spine, widest at the posterodorsal end and with a diagonal dorsal surface, facing anterodorsally (Fig. 5), alike in the holotype of *M. longicollum* (Mateus *et al.,* 2009). A similar gradual expansion from approximately half the height of the neural spine to a bulbous distal end is present in *D. armatus* (Galton, 1985; Sánchez-Fenollosa *et al*., 2024) and in two anterior dorsal spines of *T. atlasicus,* but in the latter it is widest in the anterodorsal part of the apex (Zafaty *et al.,* 2024). This differs from the condition in the mid-dorsal neural spines in *H. mjosi* and *S. stenops* (Carpenter *et al*., 2001; Maidment *et al*., 2015, 2018), where some distal expansion of the neural spine may be present, but much less developed transversely, only on the very distal end (approximately last 10th of the neural spine height) and as a mostly flat sub-horizontal and dorsoventrally thin surface perpendicular to the neural spine shaft (Maidment *et al*., 2015).

Anterior caudal vertebrae

Caudal vertebrae (Cd) 8 and 9 have been freed from matrix, and various neural arch fragments (pedicels, zygapophyses, caudal ribs and partial neural spines) were reassembled to Cd8 to Cd13 after further preparation (Figs. 8-10). The anterior caudal centra of MG 4863 (like all other caudal centra preserved in the specimen; Costa and Mateus, 2019) are wider transversely than tall dorsoventrally, and taller dorsoventrally than long anteroposteriorly, with sub-circular to heart-shaped outlines in anterior or posterior view (Figs. 8-10). This is similar to the condition in the anterior and mid-caudal centra of *D. armatus* (Galton, 1985; Sánchez-Fenollosa *et al*., 2024).

The sharp decrease in size of the most posterior of the proximal caudal neural spines of MG 4863 (Costa and Mateus, 2019) is further evidenced by the additional preparation of the neural arch of Cd11 (Tab. 2; for other measurements of these and other caudal vertebrae of the specimen, see Costa and Mateus, 2019). In Cd10 the neural spine is longer proximodistally than the centrum is tall dorsoventrally, and the shaft is ellipsoid in cross section, transversely thick and dorsoventrally deeper; the spine in Cd11 appears to have had a similar morphology, but in contrast to that of Cd10, it is half as wide and deep (but incomplete distally, so its proximodistal length is uncertain); and in Cd12 the neural spine is low dorsoventrally and transversely thin (similarly to the less

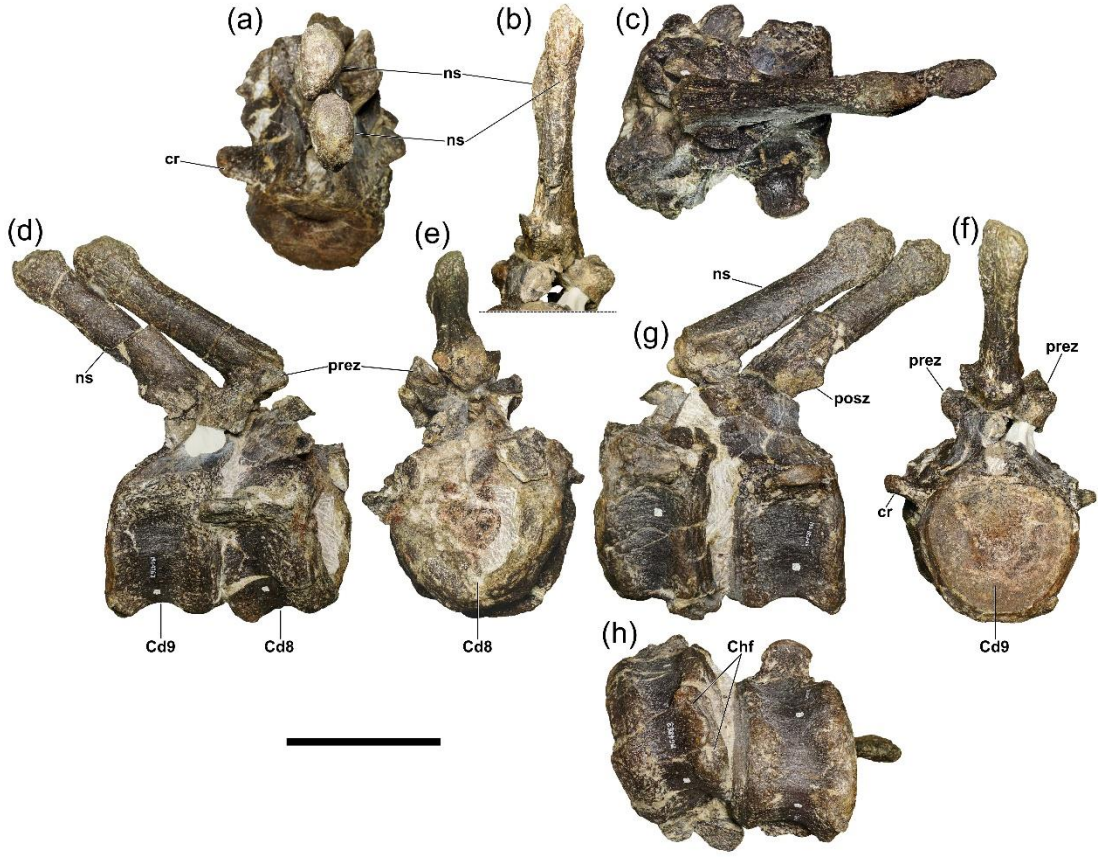

Figure 8. Caudal vertebrae eight and nine of *Miragaia longicollum* MG 4863. In (a) posterodorsal, (b) posteroventral, (c) dorsal, (d) right lateral, (e) anterior, (f) posterior, (g) left lateral, and (h) ventral views; (b), detail of neural spines; key: Cd8, caudal vertebra 8; Cd9, caudal vertebra 9; chf, chevron facets; cr, caudal rib; ns, neural spine; posz, postzygapophyses; prez, prezygapophyses; scale bar equal to 10 cm.

Figura 8. Vértebras caudais oito e nove de *Miragaia longicollum* MG 4863. Em vista (a) dorso-posterior, (b) ventroposterior, (c) dorsal, (d) lateral direita, (e) anterior, (f) posterior, (g) lateral esquerda e (h) ventral; (b), pormenor dos espinhos neurais; Cd9, vértebra caudal nove; chf, facetas chevron; cr, costela caudal; ns, espinha neural; posz, pós-zigapófises; prez, pré-zigapófises; Cd8, vértebra caudal oito; barra de escala igual a 10 cm.

Table 2. Measurements of anterior caudal vertebrae of *Miragaia longicollum* MG 4863. Cd, caudal vertebrae; values represent the maximum measurement; ( ) incomplete measurement (inferior to actual measurement if fossil was complete); * estimated measurement; values in mm.

Tabela 2. Medidas das vértebras caudais anteriores de *Miragaia longicollum* MG 4863. Cd, vértebras caudais; os valores representam a medida máxima; ( ) medida incompleta (inferior à medida real se o fóssil estivesse completo); * medida estimada; valores em mm.

	Centum height	Neural spine height	Neural spine length	Neural spine width	Apex of neural spine length	Apex of neural spine width
Cd1	99,5	(108) 130*	43	13,5	-	-
Cd5	90,5	(89) 130*	28	24	-	-
Cd8	99	165	28,7	19	39,4	25,5
Cd9	97	156	28	16	36,2	21,1
Cd10	89	(92) 115*	23	14,5	-	-
Cd12	90	21	46	9	4	-
Cd13	91	-	35	8	-	-

complete one in Cd13), half-circle shaped in lateral view (Fig. 10c, f; Tab. 2); and vestigial to absent further posteriorly in the anterior caudal series (Costa and Mateus, 2019: figures 36b, e, 38, 39). This condition is not known to occur in any other stegosaur, where caudal neural spines decrease in size progressively passing posteriorly down the caudal series, and generally neural spines are still quite elongate in the mid-caudal vertebrae, disappearing only by Cd33-35 (e.g., *S. stenops*, *L. priscus*, *K. aethiopicus*; Galton, 1985, 1991; Galton and Upchurch, 2004; Gilmore, 1914; Hennig, 1925; Maidment *et al*., 2015; Mallison, 2010, 2011). In the holotype of *D. armatus,* two mid-caudal vertebrae preserve elongate and transversely wide neural spines (Galton, 1985: vertebrae identified as P and Q in figures 4a, 5a, 6a and 12w), indicating that *D. armatus* possessed a condition more like other stegosaur taxa than MG 4863.

The preparation of the neural spine of Cd11 also demonstrates that the increasingly posteriorly angled neural spines passing posteriorly observed in the anterior caudal vertebrae of MG 4863 is a natural condition (not the result of deformation of the anterior caudal vertebrae; Figs. 9, 10; Costa and Mateus, 2019: figures 26, 30), as its preserved proximal section reaches bellow 45º to the horizontal by this vertebra. This differs from the condition in other thyreophorans, where neural spines generally retain a mostly constant vertical to slightly posterodorsal orientation, decreasing in size and flattening out only in the posterior caudal vertebrae (*e.g.*: *S. stenops, Scelidosaurus harrisonii* Owen, 1861*, H. mjosi, D. armatus*, *C. jiangbeiensis;* Carpenter *et al.,* 2001; Galton, 1985; Galton and Upchurch, 2004; Maidment *et al.,* 2015; Sánchez-Fenollosa *et al*., 2024: figures 6, 7; NHMUK PV OR 46013), or become increasingly anteriorly oriented passing posteriorly in the caudal series (as in *K. aethiopicus* and *L. priscus;* Galton, 1985, 1990; Hennig, 1925; Mallison, 2010, 2011).

The new preparation also reveals that the anterior caudal ribs of MG 4863 become progressively more dorsally oriented extending posteriorly in the caudal series, from mostly laterally projecting in Cd3-Cd5, to projecting dorsolaterally by Cd11-Cd13 (Figs. 8-10). This contrasts with the condition in *D. armatus,* where the anterior caudal ribs increasingly curve ventrally, from mostly horizontally projecting in Cd1 to projecting ventrolaterally at 45º by Cd5-6 (Galton, 1985; Sánchez-Fenollosa *et al*., 2024), similarly to most other stegosaur taxa (*e.g., S. stenops*, *K. aethiopicus*, *H. mjosi, G. sichuanensis* and *C. jiangbeiensis*; Carpenter *et al,* 2001; Dong *et al.*, 1983; Gilmore, 1914; Hao *et al*., 2018; Hennig, 1925; Maidment *et al.,* 2008; Ostrom and McIntosh, 1966). The caudal ribs from Cd8 to Cd13 of MG 4863 lack proximodorsal processes, present in more anterior caudals of the specimen (Costa and Mateus, 2019: figures 27, 29, 30) and many stegosaur taxa such as *D. armatus*, *S. stenops* and *K. aethiopicus* (Galton and Upchurch, 2004).

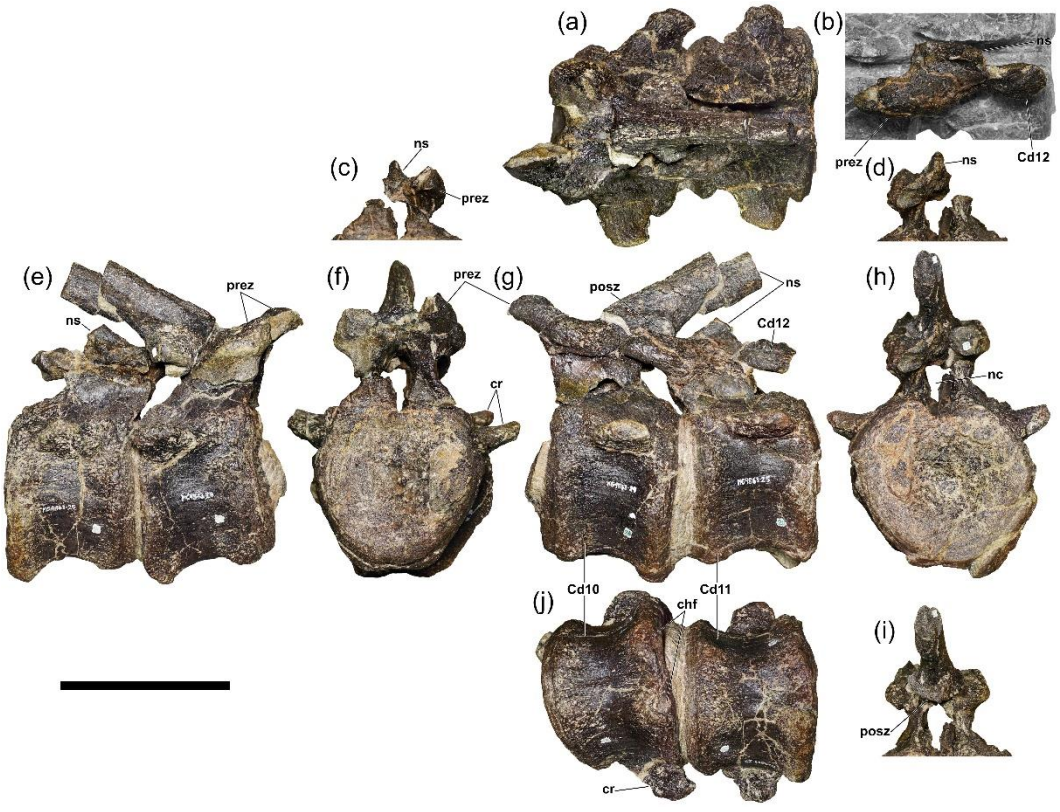

Figure 9. Caudal vertebrae 10 and 11 of *Miragaia longicollum* MG 4863. In (a, b) dorsal, (c, f) anterior, (d, h, i) posterior, (e) right lateral, (g) left lateral, and (j) ventral views; (b-d) detail of neural arch of Cd11; (i) detail of neural arch of Cd10; key: Cd10, caudal vertebra 10; Cd11, caudal vertebra 11; Cd12, caudal vertebra 12; chf, chevron facets; cr, caudal rib; nc, neurocanal; ns, neural spine; posz, postzygapophyses; prez, prezygapophyses; scale bar equal to 10 cm.

Figura 9. Vértebras caudais 10 e 11 de *Miragaia longicollum* MG 4863. Em vista (a, b) dorsal, (c, f) anterior, (d, h, i) posterior, (e) lateral direita, (g) lateral esquerda e (j) ventral; (b-d) pormenor do arco neural do Cd11; (i) pormenor do arco neural do Cd10; Cd10, vértebra caudal 10; Cd11, vértebra caudal 11; Cd12, vértebra caudal 12; chf, facetas chevron; cr, costela caudal; nc, neurocanal; ns, espinha neural; posz, pós-zigapófises; prez, pré-zigapófises; barra de escala igual a 10 cm.

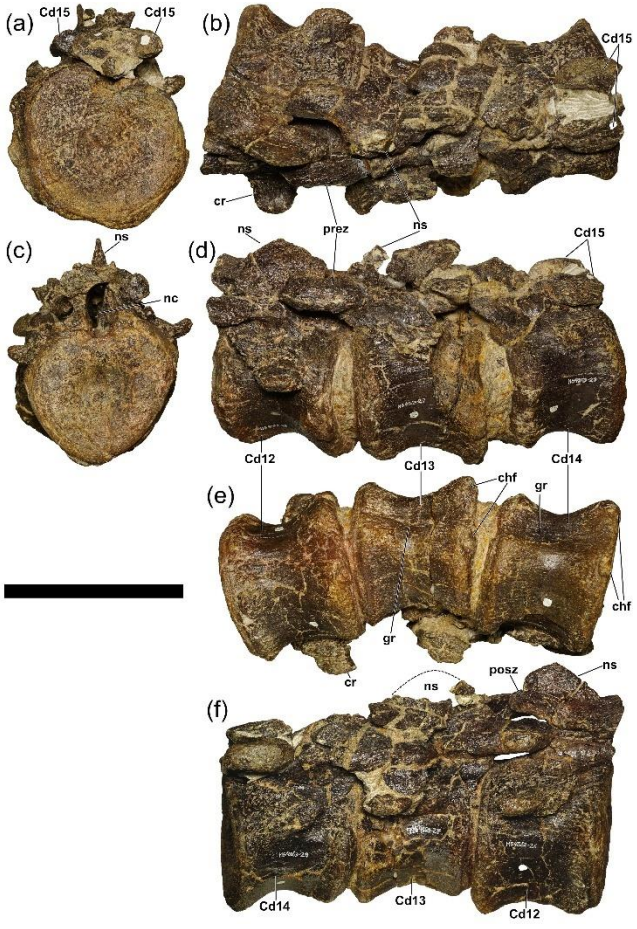

Figure 10. Caudal vertebrae 12 to 14 of *Miragaia longicollum* MG 4863. In (a) posterior, (b) dorsal, (c) anterior, (d) left lateral, (e) ventral, and (f) right lateral views; key: Cd12, caudal vertebra 12; Cd13, caudal vertebra 13; Cd14, caudal vertebra 14; Cd15, prezygapophyses of caudal vertebra 15; chf, chevron facets; cr, caudal rib; gr, groove; ns, neural spine; posz, postzygapophyses; prez, prezygapophyses; scale bar equal to 10 cm.

Figura 10. Vértebras caudais 12 a 14 de *Miragaia longicollum* MG 4863. Em vista (a) posterior, (b) dorsal, (c) anterior, (d) lateral esquerda, (e) ventral e (f) lateral direita; chf, facetas chevron; cr, costela caudal; gr, sulco; ns, espinha neural; posz, pós-zigapófises; prez, pré-zigapófises; Cd12, vértebra caudal 12; Cd13, vértebra caudal 13; Cd14, vértebra caudal 14; Cd15, pré-zigapófises da vértebra caudal 15; barra de escala igual a 10 cm.

The apices of the anterior caudal neural spines of MG 4863 are more expanded anteroposteriorly than transversely (Tab. 2; Fig. 8a-d, f), which is the reverse of the condition of most stegosaurs, such as *S. stenops, K. aethiopicus* (Galton and Upchurch 2004; Maidment *et al*., 2008), and *D. armatus* (Galton, 1985: page 218, figures 5h, 8a-c; Owen, 1875; Sánchez-Fenollosa *et al*., 2024), where neural spine apices are wider transversely than long anteroposteriorly, often with no considerable anteroposterior expansion beyond the shaft margin. In *G. sichuanensis, H. taibaii,* and *L. priscus*, anterior caudal neural spine apices are unexpanded (Galton and Upchurch, 2004; Hao *et al*., 2018; NHMUK PV R3167). The shafts of the anterior caudal neural spines of MG 4863 are also compressed transversely, similarly to *L. priscus* (NHMUK PV R3167), but opposite to *D. armatus*, where these are wider transversely than long anteroposteriorly (NHMUK PV OR 46013; Galton, 1985: figure 8).

Posterior caudal vertebrae

MG 4863-102 is the most posterior caudal vertebra of the specimen, identified as the 37th, and it was further prepared by removal of matrix and the reattachment of part of the neural arch (Fig. 11; Costa and Mateus, 2019: figure 48). As in the distal caudal vertebrae of other stegosaurs, Cd 37 is smaller than more anterior vertebrae, has flat articular facets, and less distinct chevron facets (Fig. 11).

In anterior or posterior views, the caudal centrum of Cd37 is rounded in outline with the neural canal excavating a semi-circular concavity in the dorsal surface, and markedly concave ventral surface between the chevron facets ("apple-shaped" *sensu* Costa and Mateus, 2019; figure 11c, e). This ventral groove is bordered by two low but distinct keels that extend longitudinally from each chevron facet (Fig. 11f). The mid and posterior caudal centra of MG 4863 are all shaped like this, with the dorsal and ventral excavations becoming deepest the most posteriorly in the caudal series (by Cd8 the ventral groove is already clearly present but subtle; Costa and Mateus, 2019: figures 36-48; Figs. 8-12), unlike all the anterior and mid caudal centra of *D. armatus* which are smoothly round and convex ventrally (NHMUK PV OR 46013; Galton, 1985: figure 2o, vertebrae P-R in 4A, 8D-H, M, N, 12U-X; Sánchez-Fenollosa *et al*., 2024: figures 6, 7). The posterior caudal vertebrae of *D. armatus* (Galton, 1985: I and H in figures 4a, 5a, 14b) in anterior or posterior view are uniformly rounded, as the neural canals do not excavate the centra dorsally, and the ventral surfaces are roundly convex (NHMUK PV OR 46013). The distinctive outline of the posterior caudal centra of MG 4863 is also not present in a specimen recently referred to *D. armatus* (Sánchez-Fenollosa *et al*., 2024) as the ossified chevron processes in a mid-caudal vertebra were misidentified as this feature, while the ventral surface and anterior chevron facet are smoothly round and convex (Sánchez-Fenollosa *et al*., 2024: figures 7k-o). Uniquely among stegosaurs, ossified chevrons facets fused to the respective chevrons are present in some of the anterior and mid caudal vertebrae of *D. armatus* (Galton, 1985: figures 7h-j, 8j-o; Owen, 1875: pl. 16, figures 1-3; Raven *et al*., 2023; NHMUK PV OR 46013), while this condition is not present in any of the 25 caudal vertebrae of MG 4863. In most other stegosaurs, posterior caudal centra are sub-pentagonal (when a keel is evident ventrally) or sub-hexagonal (when the ventral surface is flatter or more rounded) in outline (e.g. *S. stenops, L. priscus, H. mjosi;* Galton and Carpenter, 2016; Gilmore, 1914; Ostrom and McIntosh, 1966; Maidment *et al*., 2008, 2015).

The centrum of Cd37 is wider transversely than tall dorsoventrally, and taller dorsoventrally than it is long anteroposteriorly (as in all other caudal centra of MG 4863: Costa and Mateus, 2019: Tab. 2). These are the same proportions as the posterior caudal centra of *M. longispinus* (Galton and Carpenter, 2016; Gilmore, 1914; Costa and Mateus, 2019) and mid and posterior caudal centra of *D. armatus* (NHMUK PV OR 46013; Sánchez-Fenollosa *et al*., 2024). These proportions are the opposite of almost every other stegosaur (e.g., *S. stenops*, *H. mjosi, H. taibaii, L. priscus, C. jiangbeiensis* and *T. multispinus*; Carpenter *et al.,* 2001; Dong *et al.*, 1977, 1982, 1983; Galton, 1980; Maidment *et al.,* 2015) where the centra are transversely compressed, so the anteroposterior length exceeds the dorsoventral height, which exceeds the transverse width (Galton and Carpenter, 2016). A slight variation to this is in *B. primitivus,*

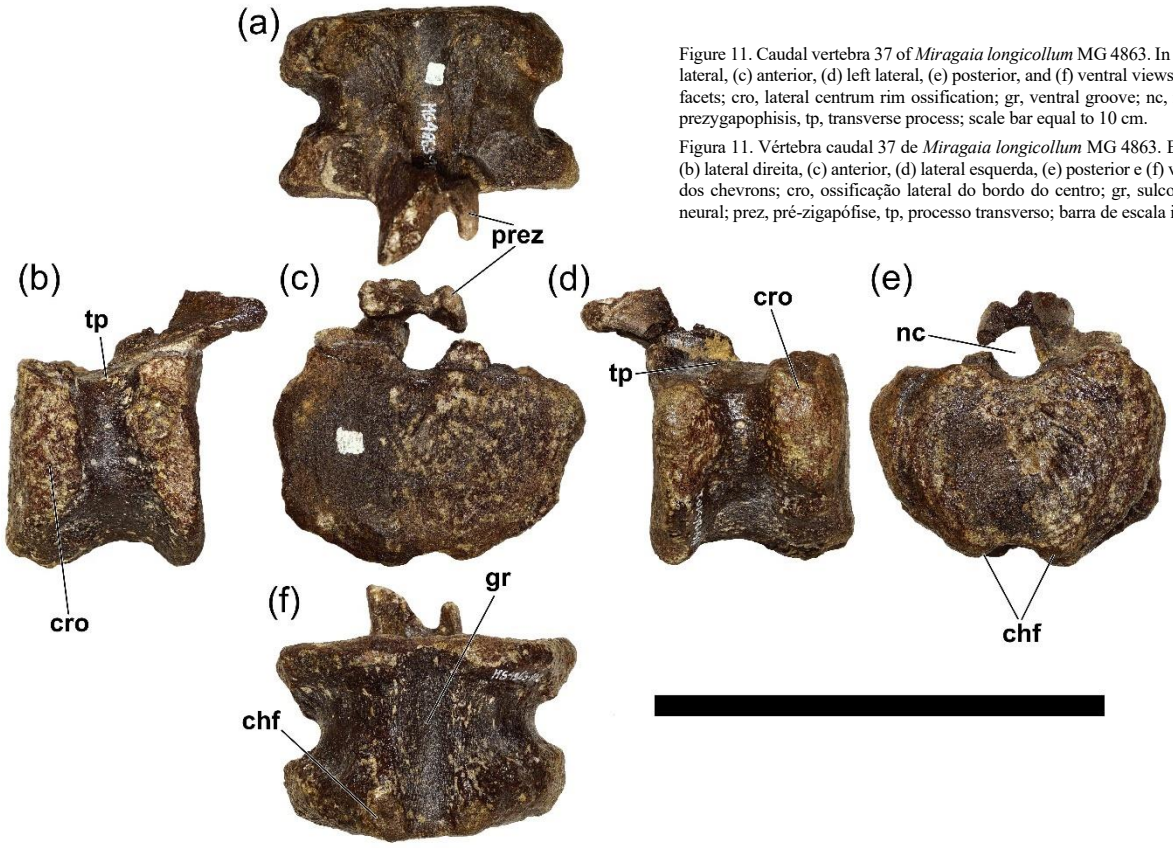

Figure 11. Caudal vertebra 37 of *Miragaia longicollum* MG 4863. In (a) dorsal, (b) right lateral, (c) anterior, (d) left lateral, (e) posterior, and (f) ventral views; key: chf, chevron facets; cro, lateral centrum rim ossification; gr, ventral groove; nc, neural canal; prez, prezygapophisis, tp, transverse process; scale bar equal to 10 cm.

Figura 11. Vértebra caudal 37 de *Miragaia longicollum* MG 4863. Em vista (a) dorsal, (b) lateral direita, (c) anterior, (d) lateral esquerda, (e) posterior e (f) ventral; chf, facetas dos chevrons; cro, ossificação lateral do bordo do centro; gr, sulco ventral; nc, canal neural; prez, pré-zigapófise, tp, processo transverso; barra de escala igual a 10 cm.

where the centrum of the single middle caudal vertebra preserved is as tall dorsoventrally as it is wide transversely, but its anteroposterior length exceeds both of these dimensions (Dai *et al.*, 2022).

Cd37 has deeply and smoothly concave lateral sides in dorsal and lateral views (as in all other mid and posterior caudal centra of MG 4863; Fig. 11; Costa and Mateus, 2019: figures 36-48). This contrasts with most stegosaurs, which have a longitudinal lateral ridge at centrum mid-height in mid and posterior caudal centra (Maidment *et al*., 2015; Raven *et al.,* 2023). Among stegosaurs, mid and/or posterior caudal centra with deeply concave lateral sides are only otherwise known in *D. armatus* and *M. longispinus* (Galton, 1985; Galton and Carpenter, 2016; Gilmore, 1914; Sánchez-Fenollosa *et al*., 2024).

Cd37 has transverse processes in the form of low ridges, partially broken but similar to those in Cd36 (Fig. 11b, d; Costa and Mateus, 2019: figure 47), so MG 4863 had transverse processes present distally on the tail, alike *M. longispinus* (Costa and Mateus, 2019; Galton and Carpenter, 2016). This differs from all other known thyreophorans, where transverse processes are absent at least in the posterior third of the tail. *H. mjosi* evidences the closest condition to MG 4863, as transverse processes are present to Cd33, while in *K. aethiopicus* these are present until Cd29 (Carpenter *et al.,* 2001; Galton and Upchurch, 2004; Maidment *et al.,* 2008, 2015). In other thyreophorans these appear to have been lost more proximally: in *S. harrisonii* they are present until Cd21, while *S. stenops, H. taibaii, L. priscus, C. jiangbeiensis, Scutellosaurus lawleri* Colbert, 1981*, T. multispinus* and *B. primitivus* lost them by Cd18 (Breeden *et al.,* 2021; Dai *et al*., 2022; Galton and Carpenter, 2016; Galton and Upchurch, 2004; Maidment *et al.,* 2015; Mallison, 2010; Norman, 2019). All the posterior caudal vertebrae preserved of *D. armatus* lack transverse processes (Galton, 1985: page 220; NHMUK PV OR 46013).

The lateral thickening of the centrum rims of Cd37 (mainly in the posterior rim, expanding anteriorly from both lateral sides; Fig. 11b, d) is more evident after preparation, alike that in Cd36 of the specimen, and the most posterior caudal centra of *M. longispinus* (Costa and Mateus, 2019; Galton and Carpenter, 2016). Similar expansion and even ankylosing are present in the posteriormost caudal centra of *K. aethiopicus* (Mallison, 2010, 2011), but absent in the posterior caudal vertebrae of *D. armatus* (NHMUK PV OR 46013).

The neural arch of Cd37, like all posterior and mid-caudal vertebrae of MG 4863, it is about one third or less the width and the height of the centrum (Costa and Mateus, 2019: figures 33-48). Measuring 20 mm in transverse width (measured from the lateral sides of the pedicels at mid-height of the neural canal) while the centrum is 64 mm wide, the reconstruction of the neural arch of Cd37 adds evidence to the gradual reduction in size of the neural arches going posteriorly in the caudal series of the specimen (Costa and Mateus, 2019). The posterior caudal vertebrae of *M. longispinus* also evidenced neural arches as narrow as those of MG 4863 (Costa and Mateus, 2019; Gilmore, 1914). Distinctively from *Miragaia,* the vertebrae in the distal two thirds of the tail of most thyreophorans have transversely wider neural arches almost as wide as the centra, so that the lateral sides of the pedicels are almost tangential with the maximum width of the centrum (e.g. *S. stenops, K. aethiopicus, D. armatus*; Galton, 1985: figures 2o, 8m, n, 12u-x; Hennig, 1925; Maidment *et al.,* 2015; Sánchez-Fenollosa *et al*., 2024: figures 7k, m).

Autopodium

MG 4863 includes one partial radiale and three left metacarpals (two of the metacarpals were semi-articulated with the radiale, but these have since been fully freed from the matrix and separated; Fig. 12a-q, s; Costa and Mateus, 2019: figure 63). All metacarpals are nearly complete and approximately equally long (and much smaller and proportionately shorter proximodistally than the four metatarsals of the same specimen; Costa and Mateus, 2019: figures 61-64, Tab. 2).

MG 4863-72 (Fig. 12g-k, m) most closely resembles the first metacarpal of *D. armatus* (Galton, 1985: figures 12a-b, 13a-b; NHMUK PV OR 46013), is proportionately the widest transversely and narrowest anteroposteriorly, although this might have been exaggerated by compression, while the proximal articular facet is broken and wholly absent.

MG 4863-71 (Fig. 12l, n-q, s) closely resembles the metacarpals identified as the second and fourth of *D. armatus* by Galton (1985: figure 12e-h) and the metacarpal from ML 433 identified as the first by Mateus *et al.* (2009), sharing a subtriangular proximal articular surface with the latter. It is slightly longer and slimmer transversely and anteroposteriorly than the other metacarpals in this specimen, more constricted just proximally from the distal articulation (which is rounded and smaller than that of the others) with subtriangular mid cross-section and proximal articular facet (the latter extending posteromedially slightly beyond the posterior margin of the distal articulation in ventral view; Fig. 12f).

MG 4863-70 (Fig. 12r, t-x) is the stockiest metacarpal, shaped like a cuboid, with a transversely wide and sub-rectangular distal articular facet, and apparently a more rounded proximal articular facet (however, this is incomplete proximoposteriorly and proximomedially, so could be more expanded in these directions). It does not resemble any of the metacarpals of *D. armatus* or *S. stenops* (Galton, 1985; Gilmore, 1914) and is most probably not the third metacarpal since these are generally the longest among stegosaurs (Galton and Upchurch, 2004). Since it is relatively symmetrical, it is also unlikely to be the fifth metacarpal, as these are generally distinctively asymmetrical, as in *D. armatus* and *S. stenops* (Galton, 1985; Ostrom and McIntosh, 1966), so it could

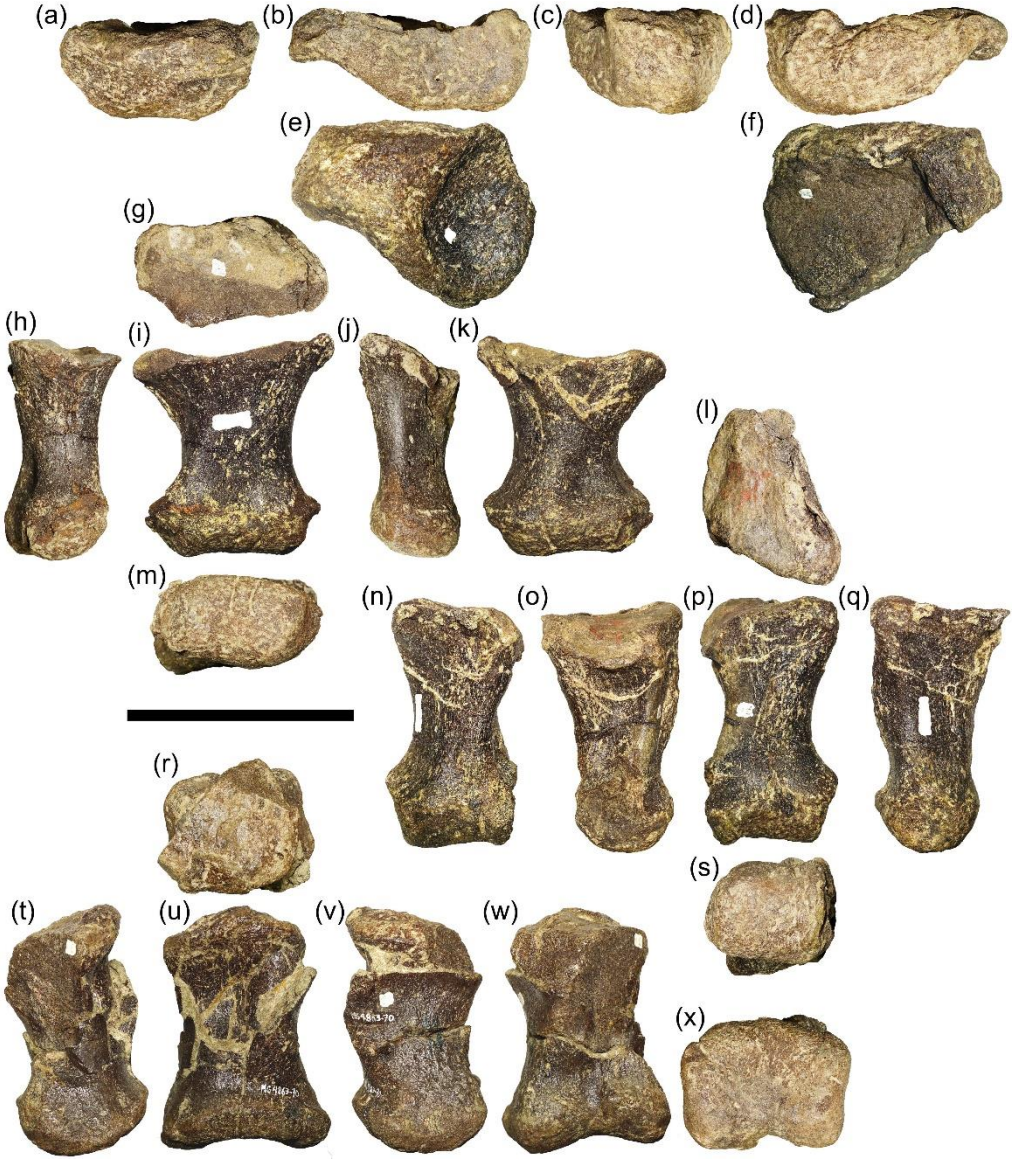

Figure 12. Left radiale and metatarsals one, two and four of *Miragaia longicollum* MG 4863. (a-f) left radiale (MG 4863-73); (g-k, m) left metacarpal one (MG 4863-72); (l, n-q, s) left metacarpal two (MG 4863-71); (r, t-x) left metacarpal four (MG 4863-70); in (a, h, o, t) medial, (b, I, p, u) anterior, (c, j, q, v) lateral, (d, k, n, w) proximal, (e, g, l, r) dorsal, and (f, m, s, x) distal views; scale bar equal to 10 cm.

Figura 12. Radial esquerdo e metatarsos um, dois e quatro de *Miragaia longicollum* MG 4863. (a-f) radiale esquerdo (MG 4863-73); (g-k, m) primeiro metacarpo esquerdo (MG 4863-72); (l, n-q, s) segundo metacarpo esquerdo (MG 4863-71); (r, t-x) quarto metacarpo esquerdo (MG 4863-70); em vista (a, h, o, t) medial, (b, I, p, u) anterior, (c, j, q, v) lateral, (d, k, n, w) proximal, (e, g, l, r) dorsal e (f, m, s, x) distal; barra de escala igual a 10 cm.

possibly be the fourth left metacarpal (instead of the first, *contra* Costa and Mateus, 2019).

The left radiale (MG 4863-73; Fig. 12a-f) is markedly concave in the purportedly ventral surface, but very incomplete dorsally, and without suture marks.

Discussion

Miragaia longicollum as a valid taxon distinct from Dacentrurus armatus

Since the first description of *Miragaia longicollum* (Mateus *et al.*, 2009), its status as a taxon distinct from the British Late Jurassic stegosaur *Dacentrurus armatus* has been called into question, mainly due to the small amount of comparable material between holotypes (Cobos *et al.*, 2010; Escaso, 2014; Ortega *et al.,* 2009). After this, a comprehensive description of *M. longicollum* MG 4863, which has widespread overlap with the holotype of *D. armatus* (NHMUK PV OR 46013), provided extensive evidence that *M. longicollum* and *D. armatus* are distinct (see Costa and Mateus, 2019). Subsequent to this, Sánchez-Fenollosa *et al.* (2024) claimed that the differences of MG 4863 from NHMUK PV OR 46013 were ambiguous and so suggested to synonymize *M. longicollum* with *D. armatus*, claiming there to be an absence of morphological criteria to distinguish these specimens and taxonomical determination. However, 17 out of the 27 previously identified differences between MG 4863 and the holotype of *D. armatus* (see Costa and Mateus, 2019: tabela 4; page 107) were omitted from that discussion (see Sánchez-Fenollosa *et al.,* 2024: page 17), and those differences omitted predominantly regard the posterior skeletal material, well represented and comparable in both specimens.

The differences of MG 4863 from the holotype of *D. armatus* exhibited in the material herein described include (condition in NHMUK PV OR 46013 between parentheses): (1) posterior midline ridge in the pedicels of the dorsal vertebrae is sharp and very consistently expanded in all dorsal vertebra (absent in all dorsal vertebrae); (2) apices of the anterior caudal neural spines more expanded anteroposteriorly than transversely (apices more expanded transversely, marginally expanded anteroposteriorly); (3) anterior caudal neural spines increasingly posteriorly oriented passing posteriorly in the caudal series, to below 45º with the horizontal by Cd8 and Cd9 (orientation of anterior caudal neural spines mostly constant and vertical to slightly posterodorsally oriented); (4) neural spines of caudal vertebrae decrease sharply in size from approximately Cd10 to Cd12, vestigial further posteriorly (gradual decrease along the caudal series, mid-caudal neural spines about as elongated as the centrum is dorsoventrally tall); (5) ribs of anterior caudal vertebrae mostly straight and progressively more dorsally oriented passing posteriorly in the caudal series, projecting dorsolaterally by Cd12 in anterior view (anterior caudal ribs progressively more ventrally oriented and curved ventrolaterally passing posteriorly, projecting ventrolaterally by the most posterior anterior caudal vertebrae); (6) neural arches of mid and posterior caudal vertebrae about a third or less the width of the centra (half or more the height and width of the centrum); (7) mid and posterior caudal centra in anterior view rounded with deeply excavating neural canal and concave ventral groove (rounded without excavation and continuously convex ventrally); (8) ossified processes in chevron facets absent in all caudal vertebrae (present in some caudal vertebrae); (9) transverse processes present until the posteriormost caudal vertebrae (absent in the posterior caudal vertebrae); (10) lateral thickening of the rims of the posteriormost caudal centra (absent).

Other differences of MG 4863 from NHMUK PV OR 46013 (but not evidenced by the material here described; see Costa and Mateus, 2019) include (condition in NHMUK PV OR 46013 between parentheses): (11) spinopostzygapophyseal laminae of cervical vertebrae extends posteriorly from the epipophyses, culminates on the anteriormost projection on the base of the neural spine with an associated medial pair of lower ridges (low and culminates posteriorly on the neural spine); (12) posterior cervical neural spines in the anterior half of the vertebra and becomes progressively more anteriorly positioned passing posteriorly in the cervical series (in the posterior half or midlength); (13) mid and posterior cervical transverse processes more than half the length of the centrum (less than half the length of the centrum); (14) outline in lateral view of cervical prezygapophyses round and close to vertical posteriorly and straight anteriorly with an anterodorsal notch (straight and close to horizontal posteriorly and round anteriorly); (15) equally as deep prepubes and proximal postpubis, obturator notch closed (postpubis approximately half as deep as postpubis, and obturator notch open); (16) ventral margin of anterior end of prepubis curves dorsally (expanded ventrally); (17) longitudinal cord-like ridges in the femur shaft present, an anterolateral one that bifurcates distally, and two posterior ones (cord-like ridges absent on the femur); (18) tibial shaft wider transversely than anteroposteriorly, and distal end not markedly expanded transversely (shaft narrower transversely than anteroposteriorly, and distal end markedly expanded transversely); (19) caudal spine with greatly expanded base, smooth concave ventral side and sharp anterior and posterior edges (spine with slightly expanded base, strongly sculpted ventral surface and rounded cross-section).

Ongoing preliminary revisions (mainly improved by comparisons with first-hand analysis of the holotype of *D. armatus;* Costa and Crespo, 2025) have found a subsequent slight reduction to 23 diagnostic differences between MG 4863 and NHMUK PV OR 46013, seven of which that also differentiate ML 433 from NHMUK PV OR 46013 (or 10 if considering ML 433-A to compliment ML 433; Costa and Crespo, 2025). The fossil record of these differing features (which include those exhibited by the newly described material herein) demonstrate that *M. longicollum* is a valid species and distinct from *D. armatus.* A specimen recently referred to *D. armatus* (Sánchez-Fenollosa *et al.,* 2024)

shares a number of features with the holotype of *D. armatus,* while being clearly distinct from MG 4863. The material newly described herein demonstrates some of these characters, including (condition in MG 4863 between parentheses): (1) orientation of anterior caudal neural spines mostly constant and predominantly vertical (anterior caudal neural spines become increasingly posteriorly oriented to below 45º with the horizontal by Cd8 and Cd9); (2) ribs of anterior caudal vertebrae progressively more ventrally oriented and curved ventrolaterally passing posteriorly, projecting ventrolaterally by the most distal anterior caudal vertebrae (anterior caudal ribs mostly straight and progressively more dorsally oriented passing posteriorly in the caudal series, projecting dorsolaterally by the most distal anterior caudal vertebrae); (3) apices of the anterior caudal neural spines more expanded transversely than anteroposteriorly (more expanded anteroposteriorly than transversely); (4) neural arches of mid and posterior caudal vertebrae half or more the height and width of the centrum (about a third or less the width of the centra); (5) mid and posterior caudal centra in anterior view rounded without excavation and continuously convex ventrally (centra rounded with deeply excavating neural canal and concave ventral groove); and (6) ossified chevron processes present (absent in all caudal vertebrae).

Given that these differing features from *M. longicollum* (while being shared with the *D. armatus* holotype) were not noted by Sánchez-Fenollosa *et al.* (2024), their identification further supports the referral of that specimen to *D. armatus*, in agreement with the authors (especially for the presence of ossified chevron processes, considered autapomorphic of *D. armatus* by various authors; *e.g.* Galton, 1985; 1991; Maidment *et al.,* 2008; Costa and Mateus, 2019; Raven *et al.,* 2023). So the CT-28 specimen mainly further corroborates the *D. armatus* holotype in how the species differed from *M. longicollum,* rather than demonstrating that these would be indistinct (*contra* Sánchez-Fenollosa *et al.,* 2024).

Observations on other dacentrurine taxa and the clade Dacentrurinae

The newly prepared material of *M. longicollum* MG 4863 also evidences a collection of features shared with a number of taxa that have been found previously within Dacentrurinae (namely *D. armatus, M. longispinus, and T. atlasicus*; Costa *et al.,* 2019; Galton and Carpenter, 2016; Mateus *et al.,* 2009; Raven *et al.,* 2023; Raven and Maidment, 2017; Zafaty *et al.,* 2024), or at least closer to *D. armatus* than *S. stenops* (namely *A. boulahfa*; Maidment *et al.,* 2020), differing from other stegosaurids that do not evidence these features (such as S. *stenops*, *L. priscus*, *H. mjosi*, *W. homheni*, *Y. ultimus* and *K. aethiopicus*; Carpenter *et al.,* 2001; Dong, 1973; Galton, 1985, 1990; Gilmore, 1914; Hennig, 1925; Jia *et al.*, 2024; Maidment *et al.*, 2015; Ostrom and McIntosh, 1966). These include: (1) dorsal centra wider than long (also present in *D. armatus, A. boulahfa and T. atlasicus*); (2) dorsal pedicels slightly more than 1.5 times the height of the centrum (also present in *D. armatus*, *A. boulahfa and T. atlasicus*); (3) dorsal transverse processes projecting dorsolaterally and closer to horizontal than vertical (also present in *D. armatus, A. boulahfa* and *T. atlasicus*); (4) posterior caudal centra wider transversely than tall dorsoventrally and taller than long anteroposteriorly (also present in *D. armatus* and *M. longispinus*); (5) mid and posterior caudal centra sub-round (also present in *D. armatus* and *M. longispinus*); (6) mid and posterior caudal centra with deeply concave lateral sides (also present in *D. armatus* and *M. longispinus*).

Features uniquely shared by MG 4863 and the holotype of *M. longispinus* (and not by other stegosaur taxa) are also further evidenced by the material newly prepared herein (supporting its placement in the *Miragaia* genus; *sensu* Costa and Mateus, 2019), namely: (1) transverse processes present in the posteriormost caudal vertebrae; (2) neural arches of antero-medial to posterior caudal vertebrae about a third or less the width and height of the centrum; (3) mid and/or posterior caudal centra rounded with deeply excavating neural canal and concave ventral groove anterior view; (4) lateral thickening of the posterior rims of the posteriormost caudal centra. Some features in this material shared as well by *D. armatus* (but not by other stegosaurids) also support the placement of *M. longispinus* in the Dacentrurinae clade, namely: (5) posterior caudal centra wider transversely than tall dorsoventrally and taller than long anteroposteriorly; (6) mid and posterior caudal centra sub-round; (7) mid and posterior caudal centra with deeply concave lateral sides. These above consist of most of the diagnostic features of *Alcovasaurus longispinus* (*sensu* Galton and Carpenter, 2016), while only two (the condylar articular facet of the femur being restricted to the distal surface, and the distal pair of tail spines being widest as approximately 25% of the longitudinal length) evidently differing from *M. longicollum*, supporting the taxonomical recombination of the former as *Miragaia longispinus* (*sensu* Costa and Mateus, 2019).

A comprehensive re-evaluation of the diagnoses of these dacentrurine taxa and the Dacentrurinae clade requires an extensive phylogenetic study that should include first hand observations of available dacentrurine specimens, as well as revisions of both characters used in previous phylogenetic analyses (*e.g.* Raven and Maidment, 2017; Raven *et al.,* 2023; Sánchez-Fenollosa and Cobos, 2025) and of more recently proposed characters (*e.g.* Costa and Mateus, 2019), which was beyond the scope of the paper herein.

Conclusions

The different forms of new historical data of the stegosaur specimen MG 4863 (after being cross referenced to assess their accuracy) allowed to clarify its exact excavation site (a roadcut approximately 1 km NE from the centre of Atouguia da Baleia, Peniche, Portugal), adjacent to which is a cross section that lastly provides specific geostratigraphical

context to the specimen, reviewing it to have been part of the latest Kimmeridgian (Late Jurassic) aged Praia da Amoreira-Porto Novo Member of the Lourinhã Formation.

The fossil material of *Miragaia longicollum* MG 4863 here described extends the useful comparable osteological information of what was already the most complete stegosaur from Europe. This increase is most significant by the dorsal vertebrae of MG 4863 being finally freed from the matrix, as this is the only fossil material shared by all the type-specimens placed within Dacentrurinae or closer to *Dacentrurus armatus* than *Stegosaurus stenops* (namely *D. armatus, M. longicollum, M. longispinus,* and especially prevalent in *Adratiklit boulahfa* and *Thyreosaurus atlasicus*).

The newly prepared material of MG 4863 (informed by new direct observations of the holotype of *D.* armatus) adds evidence to the various distinctive features of this specimen from the holotype of *D. armatus* found previously (Costa and Mateus, 2019), reinforcing that a synonymization of *M. longicollum* with *D. armatus* is unsupported by the fossil evidence. As this synonymization cannot be substantiated, this also contradicts the implementation of *Miragaia longicollum* specimens and *M. longicollum* autapomorphies in a proposed hypodigm-based diagnosis of *D. armatus* (as in Sánchez-Fenollosa *et al.,* 2024) and its use in phylogenetic studies (Sánchez-Fenollosa and Cobos, 2025), as this should result in problematic and less resolved taxonomies.

Any study of a poorly or sparsely represented fossil group points out that, to better understand its taxonomy, more complete specimens are needed to directly compare the fossil record and define shared and differing characteristics. For Late Jurassic European stegosaurs and dacentrurine stegosaurs throughout the world, this remains best achieved by MG 4863 as it is the most complete specimens in these contexts, so the additional morphological and geostratigraphical data herein has the potential to be an important contribution to many future studies.

Acknowledgments

The authors would like to thank João Paulo Zbyszewski, Teresa Zbyszewska, and Museu da Lourinhã for access to the field notebooks of G. Zbyszewski, and O. Mateus for locating and first identifying these.

The authors would like to dedicate this work to Miguel Magalhães Ramalho (1937-2021), former director of the Museu Geológico de Lisboa.

This work was supported by the National Funds through FCT - Fundação para a Ciencia e a Tecnología, I.P. (Portugal), through the grant SFRH/BD/148035/2019 and the Project PTDC/CTA-PAL/2217/2021. VDC acknowledges the Stimulus of Scientific Employment, Individual Support – 2021 Call grant by the Fundação para a Ciência e a Tecnologia (Portugal, CEECIND/03080/2021; https://doi.org/10.54499/2021.03080.CEECIND/CP1657/CT0007) and GeoBioTec. This work was founded by National funding, FCT, within the framework of GEOBIOTEC FCT-UNL UIDB/04035/2020 (https://doi.org/10.54499/UIDB/04035/2020).

References

Allain, R., Vullo, R., Rozada, L., Anquetin, J., Bourgeais, R., Goedert, J., Lasseron, M., Martin, J. E., Pérez-García, A., De Fabrègues, C. P., Royo-Torres, R., 2022. Vertebrate paleobiodiversity of the Early Cretaceous (Berriasian) Angeac-Charente Lagerstätte (southwestern France): implications for continental faunal turnover at the J/K boundary. *Geodiversitas*, **44**(25): 683-752. https://doi.org/10.5252/geodiversitas2022v44a25.

Araújo, R., Mateus, O., Walen, A., Christiansen, N., 2009. Preparation techniques applied to a stegosaurian dinosaur from Portugal. *Journal of Paleontological Techniques*, **5**: 1-23.

Breeden III, B. T., Raven, T. J., Butler, R. J., Rowe, T. B., Maidment, S. C. R., 2021. The anatomy and palaeobiology of the early armoured dinosaur *Scutellosaurus lawleri* (Ornithischia: Thyreophora) from the Kayenta Formation (Lower Jurassic) of Arizona. *Royal Society Open Science*, **8**(7): 201676. https://doi.org/10.1098/rsos.201676.

Carpenter, K., Miles, C. A., Cloward, K., 2001. New primitive stegosaur from the Morrison Formation, Wyoming. *In:* Carpenter, K. (Ed.), *The Armored dinosaurs*. Indiana University Press, 55-75.

Casanovas-Cladellas, M. L., Santafé-Llopis, J. V., Santisteban-Bové, C., 1995. *Dacentrurus armatus* (Stegosauria, Dinosauria) del Cretácico inferior de los Serranos (Valencia, España). *Revista Española de Paleontología*, **10**(2): 273-283. https://doi.org/10.7203/sjp.24155.

Cobos, A., Royo-Torres, R., Luque, L., Alcalá, L., Mampel, L., 2010. An Iberian stegosaurs paradise: The Villar del Arzobispo Formation (Tithonian–Berriasian) in Teruel (Spain). *Palaeogeography, Palaeoclimatology, Palaeoecology*, **293**(1): 223-236. https://doi.org/10.1016/j.palaeo.2010.05.024.

Colbert, E., 1981. A primitive ornithischian dinosaur from the Kayenta Formation of Arizona. *Museum of Northern Arizona Bulletin*, **53**:1-61.

Company, J., Pereda-Suberbiola, X., Ruiz-Omeñaca, J. I., 2010. New stegosaurian (Ornithischia, Thyreophora) remains from Jurassic-Cretaceous transition beds of Valencia province (Southwestern Iberian Range, Spain). *Journal of Iberian Geology*, **36**(2): 243-252.

Costa, F., Crespo, V. D., 2025. *Miragaia longicollum* is a species of stegosaur distinct from *Dacentrurus armatus*: revision of diagnostic differences by direct comparisons of holotypes. *In*: E. Vlachos *et al.* (Eds.), *Book of Abstracts of the 5th Palaeontological Virtual* Congress, 300.

Costa, F., Mateus, O., 2019. Dacentrurine stegosaurs (Dinosauria): A new specimen of *Miragaia longicollum* from the Late Jurassic of Portugal resolves taxonomical validity and shows the occurrence of the clade in North America. *PLoS ONE*, **14**(11), e0224263. https://doi.org/10.1371/journal.pone.0224263.

Costa, F., Mateus, O., 2023. New occurrences of dacentrurine stegosaurs from the Upper Jurassic of North America (Morrison Formation). *Abstract book of the XXI Encuentro de Jóvenes Investigadores en Paleontología/XXI Encontro de Jovens Investigadores em Paleontologia*, 31.

Costa, F., Silva, T., Fernandes, J., Calvo, R., Mateus, O., 2017. Retracing the history of a stegosaurian dinosaur discovery in Portugal and the importance of record-keeping in Palentology. *Abstract book of the XV Encuentro de Jóvenes Investigadores en Paleontología/XV Encontro de Jovens Investigadores em Paleontologia,* 119-124.

Dai, H., Li, N., Maidment, S. C. R., Wei, G., Zhou, Y., Hu, X., Ma, Q., Wang, X., Hu, H., Peng, G., 2022. New stegosaurs from the Middle Jurassic Lower Member of the Shaximiao Formation of Chongqing, China. *Journal of Vertebrate Paleontology*, **41**: e1995737. https://doi.org/10.1080/02724634.2021.1995737.

Dong, Z. M., 1973. Dinosaurs from Wuerho. *Institute of Paleontology and Paleoanthropology Memoir*, **11**: 45-52.

Dong, Z. M., 1993. A new species of stegosaur (Dinosauria) from the Ordos Basin, Inner Mongolia, People's Republic of China. *Canadian*

Journal of Earth Sciences, **30**(10): 2174–2176. https://doi.org/10.1139/e93-188.

Dong, Z. M., Li, X., Zhou, S. W., 1977. On the stegosaurian remain from Zigong (Tzekung), Szechuan Province. *Vertebrata PalAsiatica* **15**: 312.

Dong, Z. M., Tang, Z., Zhou, S. W., 1982. Note on the new mid-Jurassic stegosaur from Sichuan Basin, China. *Vertebrata PalAsiatica* **20**(1): 84-88.

Dong, Z. M., Zhou, S. W., Zhang, Y., 1983. Dinosaurs from the Jurassic of Sichuan. *Palaeontologica Sinica, New Series C*, **162**(23): 1-151.

Escaso, F., 2014. Historia evolutiva de los Ornithischia (Dinosauria) del Jurásico Superior de Portugal (Doctoral dissertation), *Universidad Autónoma de Madrid*, 350.

Escaso, F., Ortega, F., Dantas, P., Malafaia, E., Silva, B., Sanz, J. L., 2007. Elementos postcraneales de *Dacentrurus* (Dinosauria: Stegosauria) del Jurásico Superior de Moçafaneira (Torres Vedras, Portugal). *Cantera Paleontológica*, 157-171.

França, J. C., Zbyszewski, G., Moitinho de Almeida, F., 1960. *Notícia Explicativa da Folha 26-C Penicheda da Carta Geológica de Portugal na escala de 1:50 000.* Serviços Geológicos de Portugal, Lisboa*,* 1-33.

França, J. C., Zbyszewski, G., Moitinho de Almeida, F., 1961. *Notícia Explicativa da Folha 30-A Lourinhã da Carta Geológica de Portugal na escala de 1:50 000.* Serviços Geológicos de Portugal, Lisboa, 1-27.

Galton, P. M., 1980. Partial skeleton of *Dracopelta zbyszewskii* n. gen. and n. sp., an ankylosaurian dinosaur from the Upper Jurassic of Portugal. *Géobios*, **13**(3): 451-457.

Galton, P. M., 1982. The postcranial anatomy of stegosaurian dinosaur *Kentrosaurus* from the Upper Jurassic of Tanzania, East Africa. *Geologica et Palaeontologica*, **15**: 139-160.

Galton, P. M., 1985. British plated dinosaurs (Ornithischia, Stegosauridae). *Journal of Vertebrate Paleontology*, **5**(3): 211-254.

Galton, P. M., 1990. A partial skeleton of the stegosaurian dinosaur *Lexovisaurus* from the uppermost Lower Callovian (Middle Jurassic) of Normandy, France. *Geologica et Paleontologica*, **24**: 185–199.

Galton, P. M., 1991. Postcranial remains of the stegosaurian dinosaur *Dacentrurus* from the Upper Jurassic of France and Portugal. *Geologica et Palaeontologica*, **25**: 299-327.

Galton, P. M., 2016. Notes on plated dinosaurs (Ornithischia: Stegosauria), mostly on dermal armor from Middle and Upper Jurassic of England (also France, Iberia), with a revised diagnosis for *Loricatosaurus priscus* (Callovian, England). *Neues Jahrbuch für Geologie und Paläontologie-Abhandlungen*, **282**(1): 1-25.

Galton, P. M., Carpenter, K., 2016. The plated dinosaur *Stegosaurus longispinus* Gilmore, 1914 (Dinosauria: Ornithischia; Upper Jurassic, western USA), type species of *Alcovasaurus* n. gen. *Neues Jahrbuch für Geologie und Paläontologie-Abhandlungen*, **279**(2): 185-208. https://doi.org/10.1127/njgpa/2016/0551.

Galton, P. M., Upchurch, P., 2004. Stegosauria, 343–362. *In*: Weishampel, D. B., Dodson, P., Osmólska, H. (Eds.), *The Dinosauria (2nd edition)*. University of California Press, Berkeley. 343-362.

Gilmore, C. W., 1914. Osteology of the armored dinosaurs in the United States National Museum, with special reference to the genus *Stegosaurus*. *US Government Printing Office,* **89**:1-136.

Guillaume, A. R. D., Costa, F., Mateus, O., 2022. Stegosaur tracks from the Upper Jurassic of Portugal: new occurrences and perspectives. *Ciências da Terra/Earth Sciences Journal*, **20**(1): 37-60.

Hao, B., Zhang, Q., Peng, G., Ye, Y., You, H., 2018. Redescription of *Gigantspinosaurus sichuanensis* (Dinosauria, Stegosauria) from the Late Jurassic of Sichuan, Southwestern China. *Acta Geologica Sinica-English Edition*, **92**(2): 431-441. https://doi.org/10.1111/1755-6724.13535.

Hennig, E., 1915. *Kentrosaurus aethiopicus*, der Stegosauride des Tendaguru. *Sitzungsberichte der Gesellschaft naturforschender Freunde zu Berlin, **1915***: 219–247.

Hennig, E., 1925. *Kentrurosaurus aethiopicus*; die Stegosaurierfunde vom Tendaguru, Deutsch-Ostafrika. *Palaeontographica (Supplementbände 7)*, 101-254.

Hill, G., 1988. The sedimentology and lithostratigraphy of the Upper Jurassic Lourinhã Formation, Lusitanian Basin, Portugal. *Open University* (United Kingdom).

Hill, G., 1989. Distal alluvial fan sediments from the Upper Jurassic of Portugal: controls on their cyclicity and channel formation. *Journal of the Geological Society*, **146**(3): 539-555.

Jia, L., Li, N., Dong, L., Shi, J., Kang, Z., Wang, S., Xu, S. You, H., 2024. A new stegosaur from the late Early Cretaceous of Zuoyun, Shanxi Province, China. *Historical Biology*: 1-10. https://doi.org/10.1080/08912963.2024.2308214.

Lapparent, A. F., Zbyszewski, G., 1957. Les dinosauriens du Portugal. *Mémoire des Services Géologiques du Portugal*, **2**(Nouvelle Série): 1-131.

Li, N., Li, D., Peng, G., You, H., 2024. The first stegosaurian dinosaur from Gansu Province, China. *Cretaceous Research*, 105852. https://doi.org/10.1016/j.cretres.2024.105852.

Leinfelder, R. R., Wilson, R. C. L., 1989. Seismic and sedimentologic features of Oxfordian-Kimmeridgian syn-rift sediments on the eastern margin of the Lusitanian Basin. *Geologische Rundschau*, **78**(1): 81-104.

Maidment, S. C. R., Wei, G. B., 2006. A review of Late Jurassic stegosaurs from the People's Republic of China. *Geological Magazine*, **143**(05): 621–634. https://doi.org/10.1017/S0016756806002500.

Maidment, S. C. R., Brassey, C., Barrett, P. M., 2015. The Postcranial Skeleton of an Exceptionally Complete Individual of the Plated Dinosaur *Stegosaurus* stenops (Dinosauria: Thyreophora) from the Upper Jurassic Morrison Formation of Wyoming, USA. *PLoS ONE*, **10** (10), e0138352. https://doi.org/10.1371/journal.pone.0138352.

Maidment, S. C. R., Norman, D. B., Barrett, P. M., Upchurch, P., 2008. Systematics and phylogeny of Stegosauria (Dinosauria: Ornithischia). *Journal of Systematic Palaeontology*, **6**(4): 367–407. https://doi.org/10.1017/S1477201908002459.

Maidment, S. C. R., Raven, T. J., Ouarhache, D., Barrett, P. M., 2020. North Africa's first stegosaur: implications for Gondwanan thyreophoran dinosaur diversity. *Gondwana Research*, **77**: 82-97. https://doi.org/10.1016/j.gr.2019.07.007.

Maidment, S. C. R., Woodruff, D. C., Horner, J. R., 2018. A new specimen of the ornithischian dinosaur *Hesperosaurus mjosi* from the Upper Jurassic Morrison Formation of Montana, USA, and implications for growth and size in Morrison stegosaurs. *Journal of Vertebrate Paleontology*, **38**(1): e1406366. https://doi.org/10.1080/02724634.2017.1406366.

Mallison, H., 2010. CAD assessment of the posture and range of motion of *Kentrosaurus aethiopicus* Hennig 1915. *Swiss Journal of Geosciences*, **103**(2): 211–233. https://doi.org/10.1007/s00015-010-0024-2.

Mallison, H., 2011. Defense capabilities of *Kentrosaurus aethiopicus* Hennig, 1915. *Palaeontologia Electronica,* **14**(2): 1-25.

Manuppella G., 1999. *Noticia explicativa da folha 30-A (Lourinhã) da Carta Geológica de Portugal na escala 1:50 000*. Instituto Geológico e Mineiro. Departamento de Geologia, Lisboa,1-83.

Marsh, O. C., 1887. Principal characters of American Jurassic dinosaurs, part IX. The skull and dermal armour of *Stegosaurus*. *American Journal of Science*, **3**(34): 413-417.

Mateus, O., Maidment, S. C. R., Christiansen, N. A., 2009. A new long-necked 'sauropod-mimic' stegosaur and the evolution of the plated dinosaurs. *Proceedings of the Royal Society B: Biological Sciences*, **276**(1663): 1815-1821. https://doi.org/10.1098/rspb.2008.1909.

Mateus, O., Dinis, J., Cunha, P. P., 2017. The Lourinhã Formation: the Upper Jurassic to lower most Cretaceous of the Lusitanian Basin, Portugal–landscapes where dinosaurs walked. *Ciências da Terra/Earth Sciences Journal*, **19**(1): 75-97. https://doi.org/10.21695/cterra/esj.v19i1.355.

Mota, T. S. A., 2007. *Os Serviços Geológicos entre 1918 e 1974: da quase morte a uma nova vida*. Ph.D. thesis, Universidade Nova de Lisboa, 504.

Nopcsa, F., 1911. *Omosaurus lennieri*, un nouveau dinosaurian du Cap de la Hève. *Bulletin de la Société géologique de Normandie*, **30**: 22-42.

Norman, D. B., 2019. *Scelidosaurus harrisonii* from the Early Jurassic of Dorset, England: postcranial skeleton. *Zoological Journal of the Linnean Society*, **189**(1): 47-157. https://doi.org/10.1093/zoolinnean/zlz078.

Olshevsky, G. Ford, T. L., 1993: The origin and evolution of the stegosaurs. *DinoFrontline* (Tokyo Gakken Mook. In Japanese), **4**: 64-103.

Ostrom, J. H., McIntosh, J. S., 1966. Marsh's dinosaurs: the collections from Como Bluff. *Yale University Press*.

Ortega, F., Malafaia, E., Escaso, F., Pérez-García, A., Dantas, P., 2009. Faunas de répteis do Jurássico Superior de Portugal. *Paleolusitana*, **1**: 43-56.

Ouyang, H., 1992. Discovery of *Gigantspinosaurus sichuanensis* and its scapula spine orientation. *Abstracts and Summaries for the Youth*

Academic Symposium on New Discoveries and Ideas in Stratigraphic Paleontology, **479**.

Owen, R., 1861. Monographs on the British Fossil Reptilia from the Oolitic Formations. Part First, Containing *Scelidosaurus harrisonii* and *Pliosaurus grandis*. *Monographs of the Palaeontographical Society*, **13**(56): 1-14.

Owen, R., 1875. Monograph of the Mesozoic Reptilia, Part 2: *Bothriospondylus magnus*. *Palaeontographical Society Monograph*, **29**: 15-26.

Owen, R., 1877. Monograph on the fossil Reptilia of the Mesozoic formations (*Omosaurus*, continued). *Palaeontographical Society Monographs*, **31**: 95-97.

Pereda-Suberbiola, X., Galton, P., Torcida, F., Huerta, P., Izquierdo, L. Á., Montero, D., Pérez, G., Urién, V., 2003. First Stegosaurian Dinosaur remains from the Early Cretaceous of Burgos (Spain), with a review of Cretaceous stegosaurs. *Revista Española de Paleontología*, **2**(18): 143-150. https://doi.org/10.7203/sjp.18.2.21640.

Raven, T., Maidment, S. C. R., 2017. A new phylogeny of Stegosauria (Dinosauria, Ornithischia). *Palaeontology*, **60**(3): 401-408. https://doi.org/10.1111/pala.12291.

Raven, T. J., Barrett, P. M., Joyce, C. B., Maidment, S. C., 2023. The phylogenetic relationships and evolutionary history of the armoured dinosaurs (Ornithischia: Thyreophora). *Journal of Systematic Palaeontology*, **21**(1): 2205433. https://doi.org/10.1080/14772019.2023.2205433.

Ruiz-Omeñaca, J. I., 2000. Restos de dinosaurios (Saurischia, Ornithischia) del Barremiense Superior (Cretacico Inferior) de Castellote (Teruel) en el Museum d'Histoire Naturelle de Paris. *Mas de las Matas: Groupo de Estudios Masinos*, **19**: 10-39.

Ruiz-Omeñaca, J. I., Pereda-Suberbiola, X., Piñuela, L., García Ramos, J. C., 2013. First evidence of stegosaurs (Dinosauria: Thyreophora) in the Vega Formation, Kimmeridgian, Asturias, N Spain. *Geogaceta*, **53**: 37-40.

Sánchez-Fenollosa, S., Cobos, A, 2025. New insights into the phylogeny and skull evolution of stegosaurian dinosaurs: An extraordinary cranium fromthe European Late Jurassic (Dinosauria: Stegosauria). *Vertebrate Zoology*, **75**: 147-171. https://doi.org/10.3897/vz75.e146618.

Sánchez-Fenollosa, S., Escaso, F., Cobos, A., 2024. A new specimen of *Dacentrurus armatus* Owen, 1875 (Ornithischia: Thyreophora) from the Upper Jurassic of Spain and its taxonomic relevance in the European stegosaurian diversity. *Zoological Journal of the Linnean Society*, zlae074. https://doi.org/10.1093/zoolinnean/zlae074.

Taylor, A. M., Gowland, S., Leary, S., Keogh, K. J., Martinius, A. W., 2014. Stratigraphical correlation of the Late Jurassic Lourinhã Formation in the Consolação Sub-basin (Lusitanian Basin), Portugal. *Geological Journal*, **49**(2): 143-162. https://doi.org/10.1002/gj.2505.

Ulansky, R. E., 2014. Evolution of the stegosaurs (Dinosauria; Ornithischia). *Dinologia*, 1-35.

Wilson, J. A., 1999. A nomenclature for vertebral laminae in sauropods and other saurischian dinosaurs. *Journal of vertebrate Paleontology*, **19**(4): 639-653.

Zafaty, O., Oukassou, M., Riguetti, F., Company, J., Bendrioua, S., Tabuce, R., Charrière, A., Pereda-Suberbiola, X., 2024. A new stegosaurian dinosaur (Ornithischia: Thyreophora) with a remarkable dermal armour from the Middle Jurassic of North Africa. *Gondwana Research*, **131**: 344-362. https://doi.org/10.1016/j.gr.2024.03.009.

Zbyszewski, G., Ferreira, O. V., Manuppella, G., Assunção, C. T., 1966. *Notícia Explicativa da Folha 30-B Bombarral da Carta Geológica de Portugal na escala de 1:50.000*. Serviços Geológicos de Portugal, Lisboa, 1-91.

Zhou, S. W., 1984. The Middle Jurassic dinosaurian fauna from Dashanpu, Zigong, Sichuan, Volume 2: Stegosaurs. *Sichuan Scientific and Technological Publishing House, Sichuan*, 45-51

Appendix 1. Updated list of skeletal fossil elements of Miragaia longicollum MG 4863.

Apêndice 1. Lista actualizada dos elementos esqueléticos fósseis de Miragaia longicollum MG 4863.

Col. sub-number	Material	Taphonomy
MG 4863-1	Dentary, left	Anterior tip of left dentary
MG 4863-2	Cervical vertebra and ribs 11	Missing tip of left cervical rib
MG 4863-3	Cervical vertebra and ribs 12	Missing tip of right cervical rib
MG 4863-4	Cervical vertebra and ribs 13	Missing postzygapophyses, left side of neural arch and left rib
MG 4863-5	Axis	Almost complete, but crushed and laterally deformed
MG 4863-6	Cervical vertebra 3	Laterally deformed
MG 4863-7	Cervical vertebra and ribs 4	Missing left cervical rib and laterally deformed
MG 4863-8	Cervical vertebra and ribs 5	Anterior half of centrum and tip of right prezygapophysis
MG 4863-9	Cervical vertebra and ribs 7	Missing most of the ribs and zygapophyses, laterally deformed
MG 4863-10	Cervical vertebra and ribs 9	Missing tip of right cervical rib.
MG 4863-11	Cervical vertebra and ribs 14	Missing posterior half of right cervical rib and parts of neural arch
MG 4863-13	Dorsal vertebra 8	Missing the neural spine, prezygapophyses and left transverse process
MG 4863-14	Dorsal vertebra 4	Missing parts of neural arch
MG 4863-15	Dorsal vertebra 3	Centrum, pedicel and prezygapophyses
MG 4863-16	Dorsal vertebra 7	Severely deformed, missing the neural spine and left transverse process
MG 4863-17	Dorsal vertebra 6	Almost complete, missing prezygapophyses
MG 4863-19	Caudal vertebra 28	Centrum and pedicels
MG 4863-20	Caudal vertebra 3	Missing distal half of neural spine and most of prezygapophyses
MG 4863-21	Caudal vertebra 5	Missing distal half of neural spine and most of prezygapophyses
MG 4863-22	Caudal vertebra 8	Almost complete
MG 4863-23	Caudal vertebra 9	Almost complete
MG 4863-24	Caudal vertebra 10	Almost complete, missing tip of neural spine
MG 4863-25	Caudal vertebra 11	Almost complete, missing tip of neural spine
MG 4863-26	Caudal vertebra 12	Almost complete
MG 4863-27	Caudal vertebra 13	Almost complete
MG 4863-28	Caudal vertebra 14	Almost complete
MG 4863-29	Caudal vertebra 15	Missing most of neural arch
MG 4863-30	Caudal vertebra 16	Centrum with a pedicel
MG 4863-31	Caudal vertebra 23	Centrum
MG 4863-32	Caudal vertebra 24	Missing tip of right prezygapophysis
MG 4863-33	Caudal vertebra 27	Complete vertebra, sheared neural arch
MG 4863-34	Caudal vertebra 1	Missing tip of neural spine
MG 4863-35	Caudal vertebra 19	Missing left postzygapophysis
MG 4863-36	Caudal vertebra 34	Missing prezygapophyses
MG 4863-37	Caudal vertebra 32	Missing parts of neural arch
MG 4863-38	Caudal vertebra 2	Missing neural spine and right caudal rib
MG 4863-39	Spine, left anterior	Missing distal half
MG 4863-40	Femur, left	Missing mid-section
MG 4863-41	Femur, right	Missing distal end, proximal end broken
MG 4863-42	Tibia and tarsals, left	Complete, slightly deformed
MG 4863-43	Tibia and tarsals, right	Severely deformed, distal end broken
MG 4863-44	Fibula, left	Proximal and distal ends
MG 4863-45	Fibula, right	Missing proximal end
MG 4863-46	Plate	Posterodorsal fragment of cervical plate
MG 4863-47	Dorsal rib 7, right	Proximal and medial section
MG 4863-48	Dorsal rib 7, right	Mid-distal section
MG 4863-49	Dorsal rib 5, right	Medial section
MG 4863-50	Dorsal rib 6, right	Proximal section
MG 4863-51	Chevron, posterior (?)	Chevron blade
MG 4863-52	Chevron, anterior	Complete chevron, from caudal vertebra 17
MG 4863-53	Pubis, left	Missing end of postpubis
MG 4863-54	Indet. frag.	Possibly tip of preacetabular process of ilium
MG 4863-55	Caudal Vertebra 18	Missing right prezygapophysis
MG 4863-56	Caudal Vertebra 30	Missing parts of neural arch
MG 4863-57	Caudal Vertebra 36	Centrum and pedicels
MG 4863-58	Caudal Vertebra 7	Centrum and pedicels
MG 4863-59	Illium and sacral ribs, left	Missing preacetabular process and proximal section of sacral ribs
MG 4863-60	Cranial fragments	Various fragments, probably from dentary
MG 4863-61	Dorsal rib (?)	Fragment possibly of rib, fibula or radius
MG 4863-62	Dorsal rib 7, left	Mid-anterior section
MG 4863-63	Dorsal vertebra 2	Dorsal transverse process and postzygapophysis
MG 4863-65	Ischium, left	Iliac peduncle

Col. sub-number	Material	Taphonomy
MG 4863-66	Metatarsal 4, left	Complete metatarsal
MG 4863-67	Metatarsal 3, left	Complete metatarsal
MG 4863-68	Metatarsal 3, right	Distal half
MG 4863-69	Metatarsal 2, left	Distal half
MG 4863-70	Metacarpal 4 (?), right	Missing part of proximal half
MG 4863-71	Metacarpal 2 (?), left	Almost complete
MG 4863-72	Metacarpal 1 (?), left	Missing part of proximal surface
MG 4863-73	Radiale, right	Distal half
MG 4863-75	Dorsal rib 4, right	Proximal section
MG 4863-77	Dorsal rib 1, right	Proximal end of capitulum
MG 4863-78	Dorsal rib 5, left	Proximal fragment (tuberculum)
MG 4863-79	Dorsal rib 2, right	Proximal section
MG 4863-80	Dorsal rib 5, left	Medial section
MG 4863-81	Dorsal rib 4, right	Medial section
MG 4863-82	Dorsal rib 6, right	Mid fragment
MG 4863-83	Dorsal rib 8, right	Medial section
MG 4863-84	Dorsal rib 2, left	Proximal end of capitulum
MG 4863-85	Dorsal rib 2, left	Medial section
MG 4863-86	Dorsal rib 8, left	Medial section
MG 4863-87	Plate	Proximal fragment of a cervical plate, possibly part of MG 4863-46
MG 4863-88	Dorsal rib 1, left	Medial section
MG 4863-89	Dorsal rib 1, right	Medial section
MG 4863-90	Dorsal rib 6, right	Mid-distal fragment
MG 4863-91	Dorsal rib (?)	Fragment possibly of rib, fibula or radius
MG 4863-92	Dorsal rib 4, right	Distal end
MG 4863-93	Dorsal rib 7, left	Medial fragment
MG 4863-94	Dorsal rib (?)	Fragment possibly of rib, fibula or radius
MG 4863-95	Dorsal rib 2, left	Mid-distal fragment
MG 4863-96	Dorsal rib 6, left	Proximal fragment (tuberculum)
MG 4863-97	Dorsal rib 1, left	Mid-anterior fragment
MG 4863-98	Caudal frag.	Apex of anterior caudal neural spine, probably of Cd2 or Cd3
MG 4863-99	Dorsal rib (?)	Indeterminate fragment
MG 4863-100	Cervical rib 17, right	Medial fragment
MG 4863-101	Caudal vertebra 4	Proximal fragment of caudal rib of anterior caudal vertebra
MG 4863-102	Caudal vertebra 37	Missing parts of neural arch
MG 4863-103	Caudal frag.	Apex of anterior caudal neural spine probably from Cd4
MG 4863-104	Cervical frag.	Anterior process of cervical rib, probably of Cv10
MG 4863-105	Cervical frag.	Cervical rib fragment, probably of Cv10
MG 4863-106	Cervical frag.	Cervical right postzygapophysis from Cv13 (MG 4863-4)
MG 4863-107	Cervical frag.	Cervical rib fragment, probably of Cv3
MG 4863-108	Cervical frag.	Cervical right postzygapophysis, probably of Cv6
MG 4863-109	Indet. frag.	Indeterminate fragment, possibly cranial
MG 4863-110	Cervical frag.	Cervical rib fragment, probably of Cv5
MG 4863-113	Dorsal vertebra 9	Distal right transverse process
MG 4863-114	Indet. frag.	Possibly distal end of ischium
MG 4863-115	Indet. frag.	Possibly plate fragment
MG 4863-116	Indet. frag.	Indeterminate fragment
MG 4863-117	Indet. frag.	Possibly osteoderm fragment
MG 4863-118	Indet. frag.	Possibly osteoderm fragment
MG 4863-119	Indet. frag.	Possibly osteoderm fragment
MG 4863-120	Indet. frag.	Possibly osteoderm fragment
MG 4863-121	Indet. frag.	Possibly osteoderm fragment
MG 4863-122	Ossified tendons	Broken sections
MG 4863-123	Indet. frag.	Probably part of the pelvic girdle, most probably from the ischium
MG 4863-124	Indet. frag.	Indeterminate fragment, possibly part of rib
MG 4863-125	Indet. frag.	Probably part of the pelvic girdle
MG 4863-126	Quadrate, left	Anterior, dorsal and posterior margins incomplete
MG 4863-127	Indet. frag.	Probably part of the pelvic girdle, either from ischium or pubis
MG 4863-128	Indet. frag.	Indeterminate fragment. Possibly from *D. zbyszewskii* holotype
MG 4863-129	Indet. frag.	Indeterminate fragment, possibly osteodermic fragment
MG 4863-130	Indet. frag.	Indeterminate fragment
MG 4863-131	Indet. frag.	Possibly part of the pelvic girdle
MG 4863-132	Indet. frag.	Indeterminate fragment
MG 4863-133	Indet. frag.	Indeterminate fragment

Appendix 2. Notes of the "*Dinosaure du C. do Cervantes (Atouguia da Baleia*)" by Georges Zbyszewski. (a) cover of field notebook where the notes are included (unmarked and undated), (b) original notes (in French), (c) possible English translation of (illegible passages replaced with *, uncertain interpretations marked with " ", alternative interpretations marked with [ ]);

Apêndice 2. Notas do "*Dinosaure du C. do Cervantes (Atouguia da Baleia)*" por Georges Zbyszewski. (a) capa do caderno de campo onde se encontram estas notas (não marcado e não datado), (b) notas originais (em Francês), (c) possível tradução inglesa (passagens ilegíveis substituídas por *, interpretações incertas marcadas com " ", interpretações alternativas marcadas com [ ]);

(a)

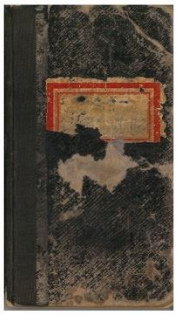

(b)

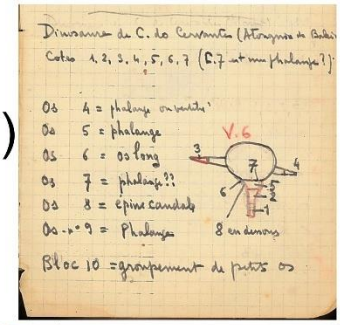

(c)

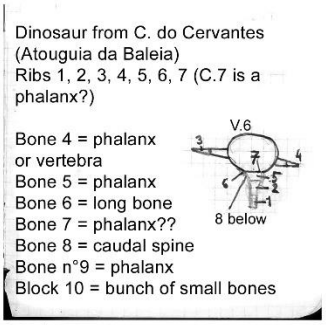

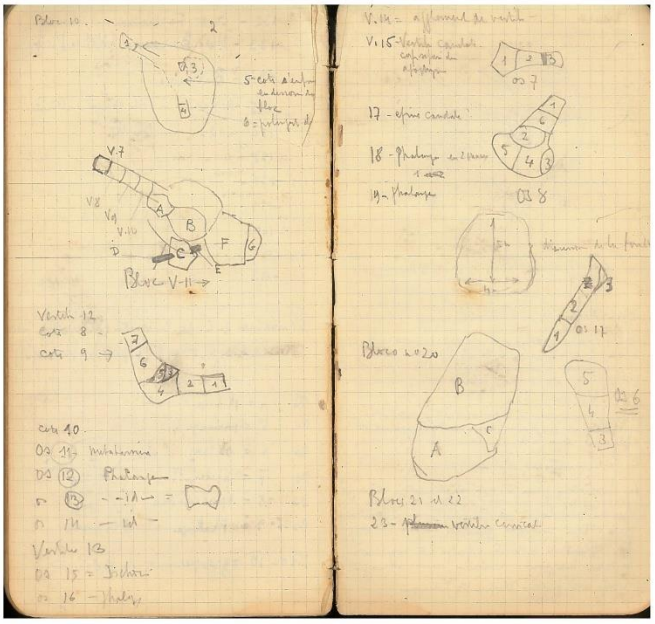

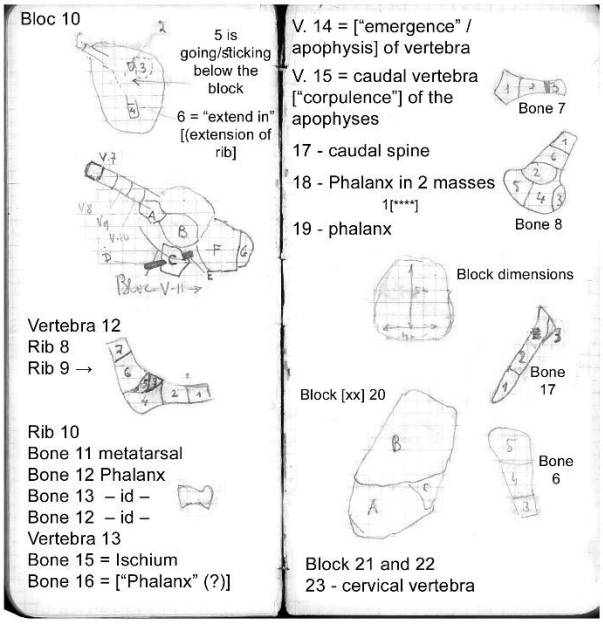

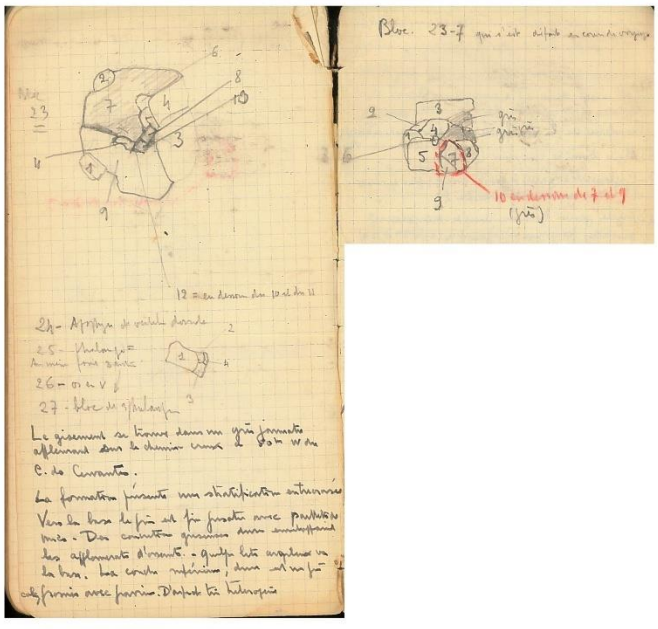

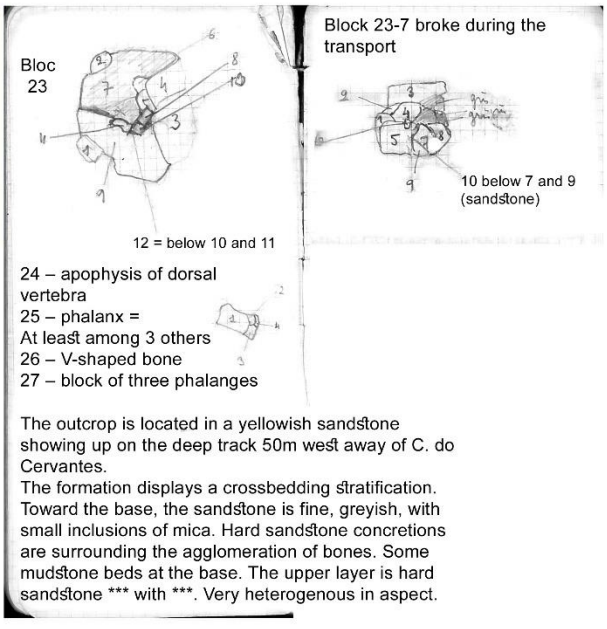

The outcrop is located in a yellowish sandstone showing up on the deep track 50m west away of C. do Cervantes.
The formation displays a crossbedding stratification. Toward the base, the sandstone is fine, greyish, with small inclusions of mica. Hard sandstone concretions are surrounding the agglomeration of bones. Some mudstone beds at the base. The upper layer is hard sandstone *** with ***. Very heterogenous in aspect.

Appendix 3. Fossils likely corresponding to those in "*Dinosaure du C. do Cervantes (Atouguia da Baleia)*", historical note about the Atouguia da Baleia skeleton, and its alleged site. (a-f), fossils of *Miragaia longicollum* MG 4863 in various states of preparation, (a) fifth caudal vertebra (in inverted posterior view) which most likely corresponds to "V.6" in Appendix 2(b); (b, d) caudal spine (prior to removal of matrix), which most likely corresponds to "Bone 8" in Appendix 2(b), with detail of distal end (b) with visible "8" marked in red crayon; (c) block marked as "23-7" in red crayon, analogous to as listed in Appendix 2 (b); (e, f) two metacarpals and one radiale most likely corresponding "27 – block with three phalanges" in Appendix 2(b), prior to (e) and after partial laboratorial preparation (f), with "27" scribed in red crayon on the sectioned dorsal surface of one of the metatarsals (MG 4863-71; see also figure 12l); (g) note dated to 28th of December of 1958 by Zbyszewski in the Actas of SGP (in Portuguese, translated as "After an interview with Professor A. de Lapparent, from *Institut Catholique de Paris*, it was arranged the preparations, in collaboration with this professor, of a second *memoir* about the Portuguese dinosaurs with the respective description primarily of the skeletal parts found in the excavations undergone near Atouguia da Baleia, in the sandstones of the Lusitanian"); (h) Luis Filipe Silva indicating the cavity where the stegosaur from Atouguia da Baleia was reportedly collected (obscured by reeds); scale bars equal 10 cm; (a-f, h) photographs by FC, 2015 (a-f) and 2023 (h).

Apêndice 3. Fósseis provavelmente correspondentes aos em "*Dinosaure du C. do Cervantes* (Atouguia da Baleia)", nota histórica sobre o esqueleto de Atouguia da Baleia, e o seu suposto sítio. (a-f), fósseis de *Miragaia longicollum* MG 4863 em vários estados de preparação, (a) quinta vértebra caudal (em vista posterior invertida), provavelmente correspondente a "V. 6" no Apêndice 2(b); (b, d) espinho caudal (antes da remoção da matriz), provavelmente correspondente ao "Osso 8" no Anexo 2(b), e pormenor da extremidade distal (b) com "8" visivelmente marcado a lápis de cera vermelho; (c) bloco assinalado como "23-7" a lápis de cera vermelho, análogo ao listado no Anexo 2(b); (e, f) dois metacarpos e um radial provavelmente correspondentes a "27 – bloco com três falanges" no Apêndice 2(b), antes de (e) e após preparação laboratorial parcial (f), com "27" inscrito a lápis vermelho na superfície dorsal seccionada de um dos metatarsos (MG 4863-71; ver também figura 12l); (g) nota datada de 28 de Dezembro de 1958 por Zbyszewski nas Actas do SGP; (h) Luis Filipe Silva indicando a cavidade onde terá sido recolhido o estegossauro de Atouguia da Baleia; Escalas correspondentes a 10cm; (a-f, h) fotografias por FC, 2015 (a-f) e 2023 (h).

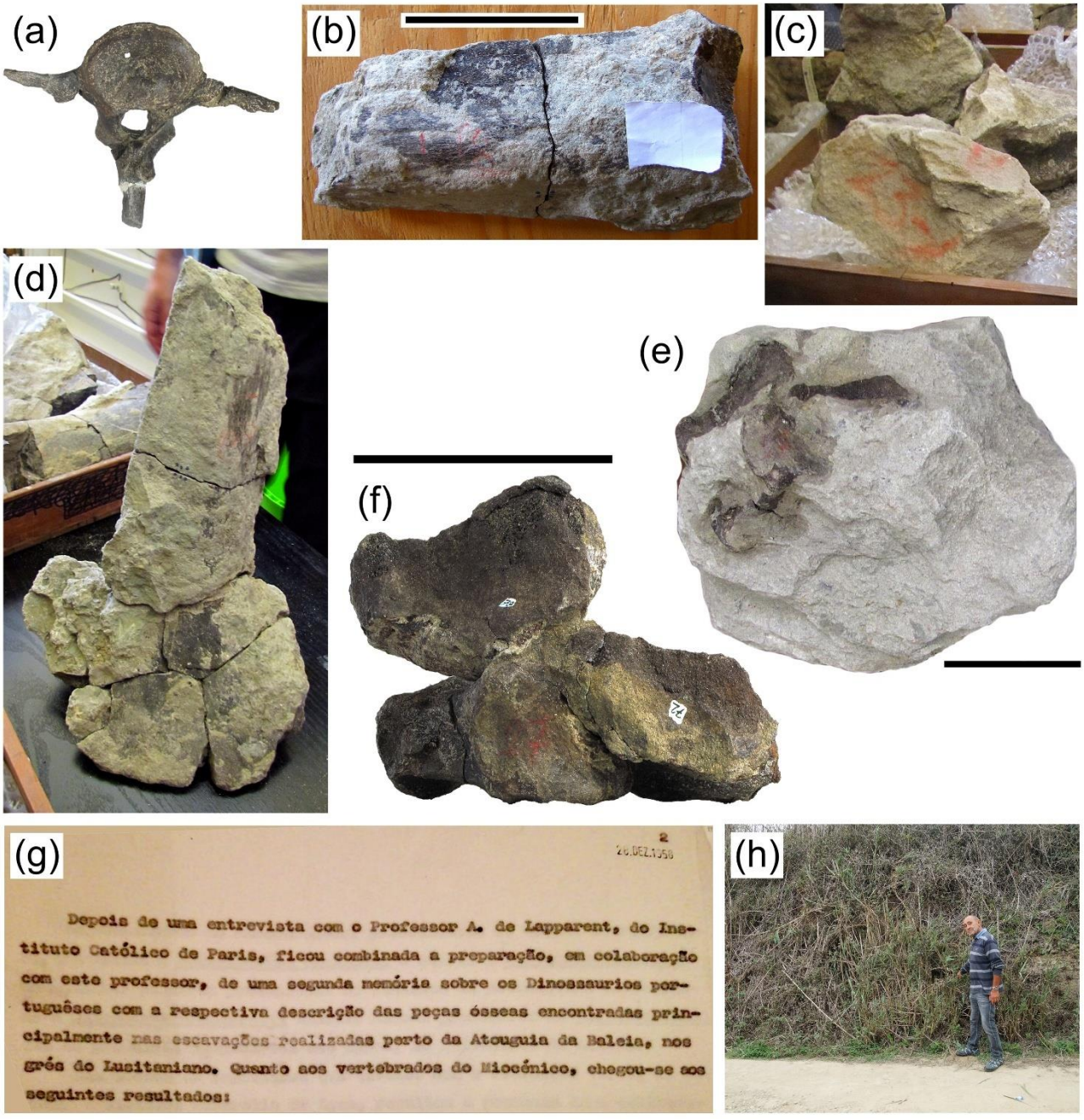

Appendix 4. Full field map of the excavation of *Miragaia longicollum* MG 4863 (Zbyszewski, circa 1958-1959).

Apêndice 4. Mapa integral da escavação de *Miragaia longicollum* MG 4863 (Zbyszewski, circa 1958-1959).